A CLUSTER OF RESULTS ON AMPLITUHEDRON TILES

CHAIM EVEN-ZOHAR, TSVIQA LAKREC, MATTEO PARISI, MELISSA SHERMAN-BENNETT, RAN TESSLER, AND LAUREN WILLIAMS

Abstract. The amplituhedron is a mathematical object which was introduced to provide a geometric origin of scattering amplitudes in $\mathcal{N} = 4$ super Yang Mills theory. It generalizes *cyclic polytopes* and the *positive Grassmannian*, and has a very rich combinatorics with connections to cluster algebras. In this article we provide a series of results about tiles and tilings of the $m = 4$ amplituhedron. Firstly, we provide a full characterization of facets of BCFW tiles in terms of cluster variables for $\mathrm{Gr}_{4,n}$. Secondly, we exhibit a tiling of the $m = 4$ amplituhedron which involves a tile which does not come from the BCFW recurrence – the *spurion* tile, which also satisfies all cluster properties. Finally, strengthening the connection with cluster algebras, we show that each standard BCFW tile is the positive part of a cluster variety, which allows us to compute the canonical form of each such tile explicitly in terms of cluster variables for $\mathrm{Gr}_{4,n}$. This paper is a companion to our previous paper "Cluster algebras and tilings for the $m = 4$ amplituhedron."

Contents

1. Introduction 1
2. Background: the amplituhedron and BCFW tiles 2
3. Background: cluster algebra and BCFW tiles 10
4. Facets of BCFW tiles 16
5. The spurion tile and tiling 29
6. Standard BCFW tiles as positive parts of cluster varieties 32
7. Canonical forms of BCFW tiles from cluster algebra 37
Appendix A. List of tiles in a spurion tiling 42
References 43

1. Introduction

The amplituhedron is a geometric object which was introduced in the context of scattering amplitudes in $\mathcal{N} = 4$ super Yang Mills theory. In particular, the fact that the *BCFW recurrence*[1] computes scattering amplitudes in $\mathcal{N} = 4$ super Yang Mills theory is a reflection of the geometric statement (which we proved in [ELP$^+$23]) that each BCFW collection of cells in the positive Grassmannian gives rise to a *tiling* of the $m = 4$ amplituhedron. The $m = 4$ amplituhedron also has a close connection to *cluster algebras*: we proved in [ELP$^+$23] that each BCFW tile satisfies the *cluster adjacency conjecture*, that is, its facets are cut out by compatible cluster variables.

[1]BCFW refers to Britto, Cachazo, Feng, and Witten

In this paper, which is a companion paper to [ELP+23], we continue our study of the cluster structure and tilings of the $m = 4$ amplituhedron. In particular, we provide a full characterization of the facets of BCFW tiles in terms of cluster variables for $\mathrm{Gr}_{4,n}$. For *standard* BCFW tiles we prove our characterization of facets, see Theorem 4.1, extending results of [ELT21]. For *general* BCFW cells we state a characterization of facets in Claim 4.25 but omit the proof, which uses the same ideas as the proof of Theorem 4.1 but is more technical.

While there are many tilings of the amplituhedron which use BCFW tiles, we show that there are also tilings that involve other tiles. In particular, we exhibit the first known tiling of an amplituhedron which uses a non-BCFW tile, the *spurion* tile.

Finally, strengthening the connection with cluster algebras, we show that each standard BCFW tile is the positive part of a cluster variety, see Theorem 6.7. In Section 7 we then use our description of BCFW tiles in terms of cluster variables for $\mathrm{Gr}_{4,n}$ in order to compute the canonical form of each such tile. The results of this paper provide computational tools to study BCFW tiles, their cluster structures, canonical forms and tilings.

The structure of this paper is as follows. In Section 2 and Section 3 we provide background on the amplituhedron and cluster algebras. In Section 4 we characterize the facets of BCFW tiles in terms of cluster variables for $\mathrm{Gr}_{4,n}$. In Section 5 we discuss the spurion tiling of the amplituhedron. In Section 6 we show that each standard BCFW tile can be thought of as the positive part of a cluster variety. Finally in Section 7 we explain how to compute the canonical form of a BCFW tile from the cluster variables.

Acknowledgements: The authors would like to thank Nima Arkani-Hamed for many inspiring conversations. TL is supported by SNSF grant Dynamical Systems, grant no. 188535. MP is supported by the CMSA at Harvard University and at the Institute for Advanced Study by the U.S. Department of Energy under the grant number DE-SC0009988. MSB is supported by the National Science Foundation under Award No. DMS-2103282. RT (incumbent of the Lillian and George Lyttle Career Development Chair) was supported by the ISF grant No. 335/19 and 1729/23. RT would like to thank Yoel Groman for discussions related to this work. LW is supported by the National Science Foundation under Award No. DMS-1854316 and DMS-2152991. Any opinions, findings, and conclusions or recommendations expressed in this material are those of the author(s) and do not necessarily reflect the views of the National Science Foundation. The authors would also like to thank Harvard University, the Institute for Advanced Study, and the 'Research in Paris' program at the Institut Henri Poincaré, where some of this work was carried out.

2. Background: the amplituhedron and BCFW tiles

2.1. **The positive Grassmannian.** The *Grassmannian* $\mathrm{Gr}_{k,n}(\mathbb{F})$ is the space of all k-dimensional subspaces of an n-dimensional vector space $\mathbb{F}^n$. Let $[n]$ denote $\{1, \ldots, n\}$, and $\binom{[n]}{k}$ denote the set of all k-element subsets of $[n]$. We can represent a point $V \in \mathrm{Gr}_{k,n}(\mathbb{F})$ as the row-span of a full-rank $k \times n$ matrix C with entries in $\mathbb{F}$. Then for $I = \{i_1 < \cdots < i_k\} \in \binom{[n]}{k}$, we let $\langle I \rangle_V = \langle i_1\, i_2\, \ldots\, i_k \rangle_V$ be the $k \times k$ minor of C using the columns I. The $\langle I \rangle_V$ are called the *Plücker coordinates* of V, and are independent of the choice of matrix representative C (up to common rescaling). The *Plücker*

embedding $V \mapsto \{\langle I\rangle_V\}_{I\in\binom{[n]}{k}}$ embeds $\mathrm{Gr}_{k,n}(\mathbb{F})$ into projective space[2] . If C has columns $v_1,\dots,v_n$, we may also identify $\langle i_1\, i_2\, \dots\, i_k\rangle$ with $v_{i_1}\wedge v_{i_2}\wedge\cdots\wedge v_{i_k}$, hence e.g. $\langle i_1\, i_2\, \dots\, i_k\rangle = -\langle i_2\, i_1\, \dots\, i_k\rangle$. In this paper we will often be working with the *real* Grassmannian $\mathrm{Gr}_{k,n} = \mathrm{Gr}_{k,n}(\mathbb{R})$. We will also denote by $\mathrm{Gr}_{k,N}$ the Grassmannians of k-planes in a vector space with basis indexed by a set $N\subset[n]$.

Definition 2.1 (Positive Grassmannian)**.** [Lus94, Pos06] We say that $V\in\mathrm{Gr}_{k,n}$ is *totally nonnegative* if (up to a global change of sign) $\langle I\rangle_V\geq 0$ for all $I\in\binom{[n]}{k}$. Similarly, V is *totally positive* if $\langle I\rangle_V>0$ for all $I\in\binom{[n]}{k}$. We let $\mathrm{Gr}_{k,n}^{\geq 0}$ and $\mathrm{Gr}_{k,n}^{>0}$ denote the set of totally nonnegative and totally positive elements of $\mathrm{Gr}_{k,n}$, respectively. $\mathrm{Gr}_{k,n}^{\geq 0}$ is called the *totally nonnegative Grassmannian*, or sometimes just the *positive Grassmannian*.

If we partition $\mathrm{Gr}_{k,n}^{\geq 0}$ into strata based on which Plücker coordinates are strictly positive and which are 0, we obtain a cell decomposition of $\mathrm{Gr}_{k,n}^{\geq 0}$ into *positroid cells* [Pos06]. Each positroid cell S gives rise to a matroid $\mathcal{M}$, whose bases are precisely the k-element subsets I such that the Plücker coordinate $\langle I\rangle$ does not vanish on S; $\mathcal{M}$ is called a *positroid*.

One can index positroid cells in $\mathrm{Gr}_{k,n}^{\geq 0}$ by (equivalence classes of) *plabic graphs* [Pos06].

Definition 2.2. Let G be a *plabic graph*, i.e. a planar bipartite graph[3] embedded in a disk, with black vertices $1,2,\dots,n$ on the boundary of the disk. An *almost perfect matching* M of G is a collection of edges which covers each internal vertex of G exactly once. The *boundary* of M, denoted ∂M, is the set of boundary vertices covered by M. The positroid associated to G is the collection $\mathcal{M}=\mathcal{M}(G):=\{\partial M : M \text{ an almost perfect matching of } G\}$.

For more details about plabic graphs relevant for this paper, see e.g. [ELP+23, Appendix A].

Both $\mathrm{Gr}_{k,n}$ and $\mathrm{Gr}_{k,n}^{\geq 0}$ admit the following set of operations, which will be useful to us.

Definition 2.3 (Operations on the Grassmannian)**.** We define the following maps on $\mathrm{Mat}_{k,n}$, which descends to maps on $\mathrm{Gr}_{k,n}$ and $\mathrm{Gr}_{k,n}^{\geq 0}$, which we denote in the same way:

- (cyclic shift) We define the *cyclic shift* as the map $\mathrm{cyc}:\mathrm{Mat}_{k,n}\to\mathrm{Mat}_{k,n}$ which sends $v_1\mapsto(-1)^{k-1}v_n$ and $v_i\mapsto v_{i-1}, 2\leq i\leq n$, and in terms of Plücker coordinates: $\langle I\rangle\mapsto\langle I-1\rangle$.
- (reflection) We define *reflection* as the map $\mathrm{refl}:\mathrm{Mat}_{k,n}\to\mathrm{Mat}_{k,n}$ which sends $v_i\mapsto v_{n+1-i}$ and rescales a row by $(-1)^{\binom{k}{2}}$, and in terms of Plücker coordinates: $\langle I\rangle\mapsto\langle n+1-I\rangle$.
- (zero column) For $J\subseteq[n]$, we define the map $\mathrm{pre}_J:\mathrm{Mat}_{k,[n]\setminus\{i\}}\to\mathrm{Mat}_{k,n}$ which adds zero columns in positions J, and in terms of Plücker coordinates: $\langle I\rangle\mapsto\langle I\rangle$.

Here, $I-1$ is obtained from $I\in\binom{[n]}{k}$ by subtracting 1 (mod n) from each element of I and $n+1-I$ is obtained from I by subtracting each element of I from $n+1$.

2.2. **The amplituhedron.** Building on [AHBC+16a, Hod13], Arkani-Hamed and Trnka [AHT14] introduced the *(tree) amplituhedron*, which they defined as the image of the positive Grassmannian under a positive linear map. Let $\mathrm{Mat}_{n,p}^{>0}$ denote the set of $n\times p$ matrices whose maximal minors are positive.

[2]We will sometimes abuse notation and identify C with its row-span; we will also drop the subscript V on Plücker coordinates when it does not cause confusion.

[3]We will always assume that plabic graphs are *reduced* [Pos06, Definition 12.5].

Definition 2.4 (Amplituhedron)**.** Let $Z \in \mathrm{Mat}_{n,k+m}^{>0}$, where $k+m \leq n$. The *amplituhedron map* $\tilde{Z} : \mathrm{Gr}_{k,n}^{\geq 0} \to \mathrm{Gr}_{k,k+m}$ is defined by $\tilde{Z}(C) := CZ$, where C is a $k \times n$ matrix representing an element of $\mathrm{Gr}_{k,n}^{\geq 0}$, and CZ is a $k \times (k+m)$ matrix representing an element of $\mathrm{Gr}_{k,k+m}$. The *amplituhedron* $\mathcal{A}_{n,k,m}(Z) \subset \mathrm{Gr}_{k,k+m}$ is the image $\tilde{Z}(\mathrm{Gr}_{k,n}^{\geq 0})$.

In this article we will be concerned with the case where $m = 4$.

Definition 2.5 (Tiles)**.** Fix k, n, m with $k+m \leq n$ and choose $Z \in \mathrm{Mat}_{n,k+m}^{>0}$. Given a positroid cell S of $\mathrm{Gr}_{k,n}^{\geq 0}$, we let $Z_S^\circ := \tilde{Z}(S)$ and $Z_S := \overline{\tilde{Z}(S)} = \tilde{Z}(\overline{S})$. We call Z_S and Z_S° a *tile* and an *open tile* for $\mathcal{A}_{n,k,m}(Z)$ if $\dim(S) = km$ and $\tilde{Z}$ is injective on S.

Definition 2.6 (Tilings)**.** A *tiling* of $\mathcal{A}_{n,k,m}(Z)$ is a collection $\{Z_S \mid S \in \mathcal{C}\}$ of tiles, such that their union equals $\mathcal{A}_{n,k,m}(Z)$ and the open tiles $Z_S^\circ, Z_{S'}^\circ$ are pairwise disjoint.

There is a natural notion of *facet* of a tile, generalizing the notion of facet of a polytope.

Definition 2.7 (Facet of a cell and a tile)**.** Given two positroid cells S' and S, we say that S' is a *facet* of S if $S' \subset \partial S$ and S' has codimension 1 in $\overline{S}$. If S' is a facet of S and Z_S is a tile of $\mathcal{A}_{n,k,m}(Z)$, we say that $Z_{S'}$ is a *facet* of Z_S if $Z_{S'} \subset \partial Z_S$ and has codimension 1 in Z_S.

Definition 2.8 (Twistor coordinates)**.** Fix $Z \in \mathrm{Mat}_{n,k+m}^{>0}$ with rows $Z_1, \ldots, Z_n \in \mathbb{R}^{k+m}$. Given $Y \in \mathrm{Gr}_{k,k+m}$ with rows $y_1, \ldots, y_k$, and $\{i_1, \ldots, i_m\} \subset [n]$, we define the *twistor coordinate* $\langle\langle i_1 i_2 \cdots i_m \rangle\rangle$ to be the determinant of the matrix with rows $y_1, \ldots, y_k, Z_{i_1}, \ldots, Z_{i_m}$.

Note that the twistor coordinates are defined only up to a common scalar multiple. An element of $\mathrm{Gr}_{k,k+m}$ is uniquely determined by its twistor coordinates [KW19]. Moreover, $\mathrm{Gr}_{k,k+m}$ can be embedded into $\mathrm{Gr}_{m,n}$ so that the twistor coordinate $\langle\langle i_1 \ldots i_m \rangle\rangle$ is the pullback of the Plücker coordinate $\langle i_1, \ldots, i_m \rangle$ in $\mathrm{Gr}_{m,n}$.

Definition 2.9. We refer to a homogeneous polynomial in twistor coordinates as a *functionary*. For $S \subseteq \mathrm{Gr}_{k,n}^{\geq 0}$, we say a functionary F has a definite sign $s \in \{\pm 1\}$ (or vanishes) on Z_S° if for all $Z \in \mathrm{Mat}_{n,k+4}^{>0}$ and for all $Y \in Z_S^\circ$, $F(Y)$ has sign s (or 0, respectively). A functionary is *irreducible* if it is the pullback of an irreducible function on $\mathrm{Gr}_{m,n}$.

We will use functionaries to describe amplituhedron tiles and to connect with cluster algebras.

2.3. **BCFW cells and BCFW tiles.** In this section we review the operation of *BCFW product* used to build BCFW cells, following [ELP+23, Section 5]. We then define BCFW cells and tiles.

Notation 2.10. Choose integers $1 \leq a < b < c < d < n$ with a, b and c, d, n consecutive. Let[4] $N_L = \{n, 1, 2, \ldots, a, b\}, N_R = \{b, \ldots, c, d, n\}$ and $B = (a, b, c, d, n)$[5]. Also fix $k \leq n$ and two nonnegative integers $k_L \leq |N_L|$ and $k_R \leq |N_R|$ such that $k_L + k_R + 1 = k$.

Remark 2.11. While it is convenient to state our results in terms of $[n]$ and $\mathrm{Gr}_{k,n}^{\geq 0}$, our results hold if we replace $[n]$ by any set of indices $N \subset [n]$, and replace 1 and n by the smallest and largest elements of N, respectively.

[4]Note that we will overload the notation and let n index an element of a vector space basis for different vector spaces; however, in what follows, the meaning should be clear from context.

[5]The 'B' stands for "butterfly."

Definition 2.12 (BCFW product)**.** Let $S_L \subseteq \mathrm{Gr}^{\geq 0}_{k_L,N_L}, S_R \subseteq \mathrm{Gr}^{\geq 0}_{k_R,N_R}$ be as in Notation 2.10, with G_L, G_R the respective plabic graphs, and let $B = (a, b, c, d, n)$ as in Notation 2.10. The *BCFW product* of S_L and S_R is the positroid cell $S_L \bowtie S_R \subseteq \mathrm{Gr}^{\geq 0}_{k,n}$ corresponding to the plabic graph in the right-hand side of Figure 1.

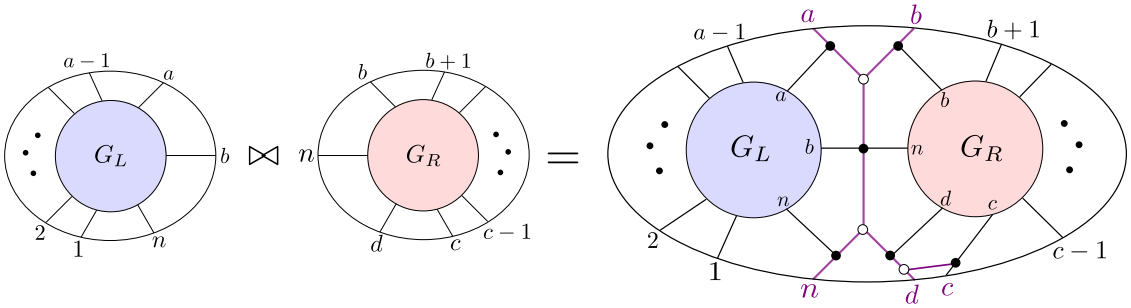

FIGURE 1. The BCFW product $S_L \bowtie S_R$ of S_L and S_R in terms of their plabic graphs. Note that G_L and G_R are joined along the purple graph associated to $B = (a, b, c, d, n)$; we call it a 'butterfly graph' since it resembles a butterfly.

When it is not clear from the context, we will say $\bowtie$ is performed 'with indices B'.

We now introduce the family of *BCFW cells* to be the set of positroid cells which is closed under the operations in Definitions 2.3 and 2.12:

Definition 2.13 (BCFW cells)**.** The set of *BCFW cells* is defined recursively. For $k = 0$, let the trivial cell $\mathrm{Gr}^{>0}_{0,n}$ be a BCFW cell. This is represented by a plabic graph with black lollipops at each of the boundary vertices. If S is a BCFW cell, so is the cell obtained by applying $\mathrm{cyc}, \mathrm{refl}, \mathrm{pre}$ to S. If S_L, S_R are BCFW cells, so is their BCFW product $S_L \bowtie S_R$.

Remark 2.14. It follows from the definition that the plabic graph of a BCFW cell is built by glueing together a collection of (possibly rotated or reflected) 'butterfly graphs.' We could therefore refer to the plabic graph of a BCFW cell as a *kaleidoscope*[6].

The *standard* BCFW cells, which we define below, are a particularly nice subset of BCFW cells. The images of the standard BCFW cells yield a tiling of the amplituhedron [ELT21].

Definition 2.15 (Standard BCFW cells)**.** The set of *standard BCFW cells* is defined recursively. For $k = 0$, let the trivial cell $\mathrm{Gr}^{>0}_{0,n}$ be a BCFW cell. If S is a BCFW cell, so is the cell obtained by adding a zero column using pre in the penultimate position. If S_L, S_R are BCFW cells, so is their BCFW product $S_L \bowtie S_R$.

Example 2.16. For $k = 1$, each BCFW cell in $\mathrm{Gr}^{\geq 0}_{1,n}$ has a plabic graph of the form shown in Figure 2 (middle). The Plücker coordinates $\langle a\rangle, \langle b\rangle, \langle c\rangle, \langle d\rangle, \langle e\rangle$ are positive, and all others are zero. In Figure 2 (right), $S_{ex} \subset \mathrm{Gr}^{\geq 0}_{2,7}$ is obtained as $S_L \bowtie S_R$, with S_L, S_R BCFW cells in $\mathrm{Gr}^{\geq 0}_{1,N_L}, \mathrm{Gr}^{\geq 0}_{0,N_R}$ respectively, with $N_L = \{7, 1, 2, 3, 4\}, N_R = \{4, 5, 6, 7\}$ and $B = (3, 4, 5, 6, 7)$. The standard BCFW cells for $k = 1$ are those BCFW cells where a, b and c, d are consecutive and $e = n$, as shown in Figure 2 (left). For $k = n - 4$, the *totally* positive Grassmannian $\mathrm{Gr}^{>0}_{n-4,n}$ is the only BCFW cell.

[6]A group of butterflies is officially called a *kaleidoscope*.

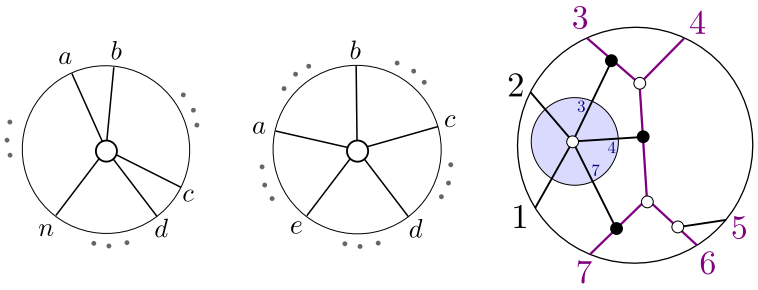

FIGURE 2. The plabic graph of a standard BCFW cell (left) and general BCFW cell (center) in $\mathrm{Gr}^{\geq 0}_{1,n}$, where the ... denote black lollipops in the remaining indices; the plabic graph of a BCFW cell $S_{ex} \subset \mathrm{Gr}^{\geq 0}_{2,7}$ (right).

In [ELP+23, Section 7] we showed that the amplituhedron map is injective on each BCFW cell. We can therefore define *BCFW tiles*.

Definition 2.17 (BCFW tiles and standard BCFW tiles)**.** We define a *BCFW tile* to be the (closure of the) image of a BCFW cell under the amplituhedron map. In other words, each BCFW tile has the form $Z_{\mathfrak{r}} := \overline{\tilde{Z}(S_{\mathfrak{r}})}$, where $\mathfrak{r}$ is a recipe. We define a *standard BCFW tile* to be a BCFW tile that comes from a standard BCFW cell.

2.4. **Standard BCFW cells from chord diagrams.** In this section we introduce *chord diagrams*, and show how each gives an algorithm for constructing a standard BCFW cell. In Section 2.5 we then give a generalization of this algorithm, called a *recipe*, for constructing a general BCFW cell.

Definition 2.18 (Chord diagram [ELT21])**.** Let $k, n \in \mathbb{N}$. A *chord diagram* $D \in \mathcal{CD}_{n,k}$ is a set of k quadruples named *chords*, of integers in the set $\{1, \ldots, n\}$ named *markers*, of the following form:

$$D \;=\; \{(a_1, b_1, c_1, d_1), \ldots, (a_k, b_k, c_k, d_k)\} \quad \text{where} \quad b_i = a_i + 1 \text{ and } d_i = c_i + 1$$

such that every chord $D_i = (a_i, b_i, c_i, d_i) \in D$ satisfies $1 \leq a_i < b_i < c_i < d_i \leq n-1$ and *no* two chords $D_i, D_j \in D$ satisfy $a_i = a_j$ or $a_i < a_j < c_i < c_j$.

The number of different chord diagrams with n markers and k chords is the Narayana number $N(n-3, k+1)$: $|\mathcal{CD}_{n,k}| = \frac{1}{k+1}\binom{n-4}{k}\binom{n-3}{k}$.

See Figure 3, where we visualize such a chord diagram D in the plane as a horizontal line with n markers labeled $\{1, \ldots, n\}$ from left to right, and k nonintersecting chords above it, whose *start* and *end* lie in the segments (a_i, b_i) and (c_i, d_i) respectively. The definition imposes restrictions on the chords: they cannot start before 1, end after $n-1$, or start or end on a marker. Two chords cannot start in the same segment $(s, s+1)$, and one chord cannot start and end in the same segment, nor in adjacent segments. Two chord cannot cross.

We say that a chord is a *top chord* if there is no chord above it, e.g. D_3 and D_6 in Figure 3. One natural way to label the chords is by $D_1, \ldots, D_k$ such that for all $1 \leq j \leq k$, D_j is the rightmost top chord among the set of chords $\{D_1, \ldots, D_j\}$ as in Figure 3. This is equivalent to sorting the chords according to their ends.

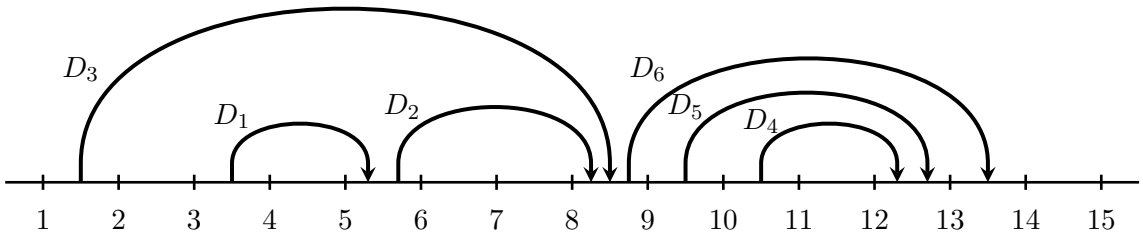

$$D = \{(3,4,5,6),(5,6,8,9),(1,2,8,9),(10,11,12,13),(9,10,12,13),(8,9,13,14)\}$$

FIGURE 3. A chord diagram D with $k = 6$ chords $n = 15$ markers.

Definition 2.19 (Terminology for chords)**.** A chord is a *top* chord if there is no chord above it, and otherwise it is a *descendant* of the chords above it, called its *ancestors*, and in particular a *child* of the chord immediately above it, which is called its *parent*. Two chords are *siblings* if they are either top chords or children of a common parent. Two chords are *same-end* if their ends occur in a common segment $(e, e+1)$, are *head-to-tail* if the first ends in the segment where the second starts, and are *sticky* if their starts lie in consecutive segments $(s, s+1)$ and $(s+1, s+2)$.

Example 2.20. Consider the chord diagram in Figure 3. D_4 has parent D_5 and ancestors D_5 and D_6. D_1 and D_2 are siblings, and D_3 and D_6 are siblings. Chords D_2 and D_3 are same-end, chords D_1 and D_2 are head-to-tail, and chords D_5 and D_6 are sticky.

Remark 2.21. The definition of a chord diagram naturally extends to the case of a finite set of markers $N \subset \{1,\dots,n\}$ rather than $\{1,\dots,n\}$, and a set K of chord indices rather than $\{1,\dots,k\}$. We will always have that the largest marker is $n \in N$, the starts and ends of chords will be consecutive pairs in N (and also $\mathbb{N}$) and the rightmost top chord will be denoted by $D_k = D_{\max K}$. The notion of chord subdiagram in Definition 2.22 is an example of this extended notion of chord diagram.

Definition 2.22 (Left and right subdiagrams)**.** Let D be a chord diagram in $\mathcal{CD}_{n,k}$. A *subdiagram* is obtained by restricting to a subset of the chords and a subset of the markers which contains both these chords and the marker n. Let $D_k = (a,b,c,d)$ be the rightmost top chord of D, where $1 \le a < b < c < d < n$, and moreover a, b and c, d are consecutive.

In the case that d, n are consecutive as well we define D_L, the *left subdiagram* of D, on the markers $N_L = \{1,2,\dots,a,b,n\}$ and the *right subdiagram* D_R on $N_R = \{b,\dots,c,d,n\}$. The subdiagram D_L contains all chords that are to the left of D_k, and D_R contains the descendants of D_k.

Example 2.23. For the chord diagram D in Figure 3, the rightmost top chord is $D_6 = (8,9,13,14)$, so $N_L = \{1,\dots,9,15\}$ and $D_L = \{D_1, D_2, D_3\}$, while $N_R = \{9,\dots,15\}$ and $D_R = \{D_4, D_5\}$.

Definition 2.24 (Standard BCFW cell from a chord diagram)**.** Let D be a chord diagram with k chords on a set of markers N. We recursively construct from D a standard BCFW cell S_D in $\mathrm{Gr}_{k,N}^{\geq 0}$ as follows:

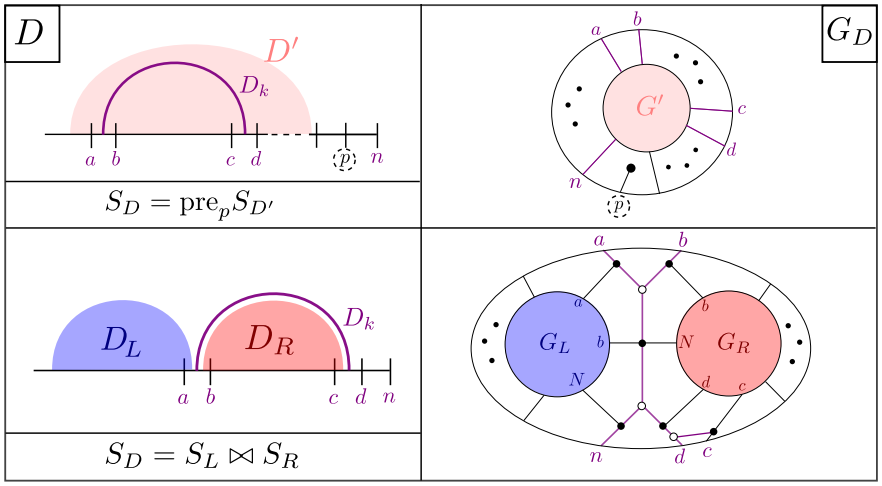

FIGURE 4. Recursive construction of a standard BCFW cell from a chord diagram as in Definition 2.24. Top left (right): construction of D (G_D) from D' (G') as in (1a); bottom left (right) construction of D (G_D) from D_L, D_R (G_L, G_R) as in (1b).

(1) If $k = 0$, then the BCFW cell is the trivial cell $S_D := \mathrm{Gr}^{\geq 0}_{0,N}$.
(2) Otherwise, let $D_k = (a, b, c, d)$ be the rightmost top chord of D and let p denote the penultimate marker in N.
   (a) If $d \neq p$, let D' be the subdiagram on $N \setminus \{p\}$ with the same chords as D, and let $S_{D'}$ be the standard BCFW cell associated to D'. Then, we define $S_D := \mathrm{pre}_p\, S_{D'}$, which denotes the standard BCFW cell obtained from $S_{D'}$ by inserting a zero column in the penultimate position p.
   (b) If $d = p$, let S_L and S_R be the standard BCFW cells on N_L and N_R associated to the left and right subdiagrams D_L and D_R of D. Then, we let $S_D := S_L \bowtie S_R$, the standard BCFW cell which is their BCFW product as in Definition 2.12.

Example 2.25. The standard BCFW cell S_D of the chord diagram D in Figure 3 is $S_L \bowtie S_R$ where the chord subdiagrams D_L, D_R are as in Example 2.23. One can keep applying the recursive definition and obtain:

$$\begin{aligned} S_L &= \mathrm{Gr}_{0,\{1,2,15\}} \bowtie \left(\left(\mathrm{Gr}_{0,\{2,3,4,15\}} \bowtie \mathrm{Gr}_{0,\{4,5,6,15\}}\right) \bowtie \mathrm{Gr}_{0,\{6,7,8,9,15\}}\right) \\ S_R &= \mathrm{pre}_{14}\left(\mathrm{Gr}_{0,\{9,10,15\}} \bowtie \left(\mathrm{Gr}_{0,\{10,11,15\}} \bowtie \mathrm{Gr}_{0,\{11,12,13,15\}}\right)\right) \end{aligned}$$

2.5. **BCFW cells from recipes.** In this section, we review the conventions for labeling general BCFW cells from [ELP+23, Section 6]. Each general BCFW cell may be specified by a list of operations from Definition 2.13. The class of general BCFW cells includes the standard BCFW cells, but is additionally closed under the operations of cyclic shift, reflection, and inserting a zero column anywhere (cf. Definition 2.13) at any stage of the recursive generation. Since any sequence of these operations can be expressed as pre_I followed by cyc^r followed by refl^s for some I, r, s, we can specify in a concise form which ones take place after each BCFW product. We will record the generation of a BCFW cell using the formalism of *recipe* in Definition 2.26.

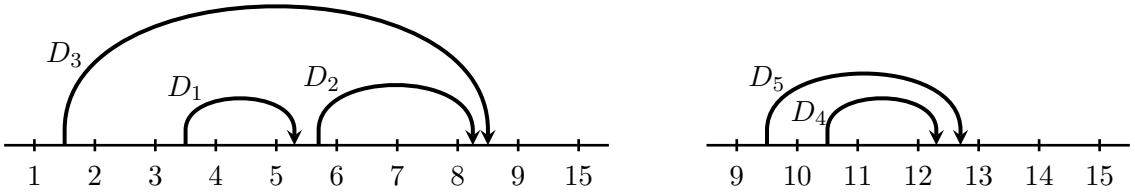

FIGURE 5. The left diagram D_L and the right diagram D_R for the chord diagram D in Figure 3.

Definition 2.26 (General BCFW cell from a recipe)**.** A *step-tuple* on a finite index set $N \subset \mathbb{N}$ is a 4-tuple

$$((a_i, b_i, c_i, d_i, n_i), \mathrm{pre}_{I_i}, \mathrm{cyc}^{r_i}, \mathrm{refl}^{s_i}),$$

where $I_i \subseteq N$ such that n_i is the largest element in $N \setminus I_i$, $a_i < b_i$ and $c_i < d_i < n_i$ are both consecutive in $N \setminus I_i$, $0 \leq r_i < |N|$, and $s_i \in \{0, 1\}$. A step-tuple records in order: a BCFW product of two cells using indices $(a_i, b_i, c_i, d_i, n_i)$; zero column insertions in positions I_i; applying the cyclic shift r_i times; applying reflection s_i times. Note that some of these operations may be the identity. Each operation in a step-tuple which is not the identity is called a *step*.

A *recipe* $\mathfrak{r}$ on N is either the empty set (the *trivial recipe* on N, denote $\mathfrak{r}_N^{\mathrm{triv}}$), or a recipe $\mathfrak{r}_L$ on N_L followed by a recipe $\mathfrak{r}_R$ on N_R followed by a step-tuple $((a_k, b_k, c_k, d_k, n_k), \mathrm{pre}_{I_k}, \mathrm{cyc}^{r_k}, \mathrm{refl}^{s_k})$ on N, where $N_L = (N \setminus I_k) \cap \{n_k, \ldots, a_k, b_k\}$ and $N_R = (N \setminus I_k) \cap \{b_k, \ldots, c_k, d_k, n_k\}$. We let $S_{\mathfrak{r}}$ denote the general BCFW cell on N obtained by applying the sequence of operations specified by $\mathfrak{r}$. If $\mathfrak{r}$ consists of k step-tuples, then $S_{\mathfrak{r}} \subset \mathrm{Gr}_{k,N}^{\geq 0}$.

Example 2.27. Consider the recipe $\mathfrak{r}$ consisting of the following sequence of 4 step-tuples:

$$((3,4,5,6,12), \mathrm{pre}_2), ((1,2,5,6,12), \mathrm{cyc}^2, \mathrm{refl})), ((6,7,8,9,11), \mathrm{pre}_{10,12}), ((5,6,10,11,12), \mathrm{cyc}^4, \mathrm{refl}).$$

Figure 6 shows the plabic graph of the general BCFW cell $S_{\mathfrak{r}}$ obtained from $\mathfrak{r}$ following Definition 2.26.

Remark 2.28 (Recipe from a chord diagram)**.** We now explain how a chord diagram D gives rise to a recipe $\mathfrak{r}(D)$. Let D be a chord diagram with k chords on a set of markers N. If $k = 0$, $\mathfrak{r}(D)$ is the trivial recipe on N. Otherwise, let (a_k, b_k, c_k, d_k) denote the rightmost top chord, let $n := \max N$, and let $I_k := \{p \in N \mid d_k < p < n\}$. Let $\overline{D}$ be the chord diagram obtained from D by removing the markers in I_k, and let D_L and D_R be the left and right subdiagrams of $\overline{D}$, on marker sets $N_L \subseteq N \setminus I_k$ and $N_R \subseteq N \setminus I_k$, respectively. Then the recipe $\mathfrak{r}(D)$ from D is recursively constructed as the recipe $\mathfrak{r}(D_L)$ followed by the recipe $\mathfrak{r}(D_R)$ followed by the step-tuple $((a_k, b_k, c_k, d_k, n), \mathrm{pre}_{I_k})$ on N.

Example 2.29. We now illustrate Remark 2.28 on the chord diagram D_L of Example 2.25, which is pictured in Figure 5. In this case we obtain the recipe

$$\mathfrak{r}_{\{1,2,15\}}^{\mathrm{triv}}, \mathfrak{r}_{\{2,3,4,15\}}^{\mathrm{triv}}, \mathfrak{r}_{\{4,5,6,15\}}^{\mathrm{triv}}, ((3,4,5,6,15)), \mathfrak{r}_{\{6,7,8,9,15\}}^{\mathrm{triv}}, ((5,6,8,9,15)), ((1,2,8,9,15)).$$

Because our arguments are frequently recursive, we need some notation for the BCFW cells obtained by deleting the final step of a recipe. We use the following notation throughout.

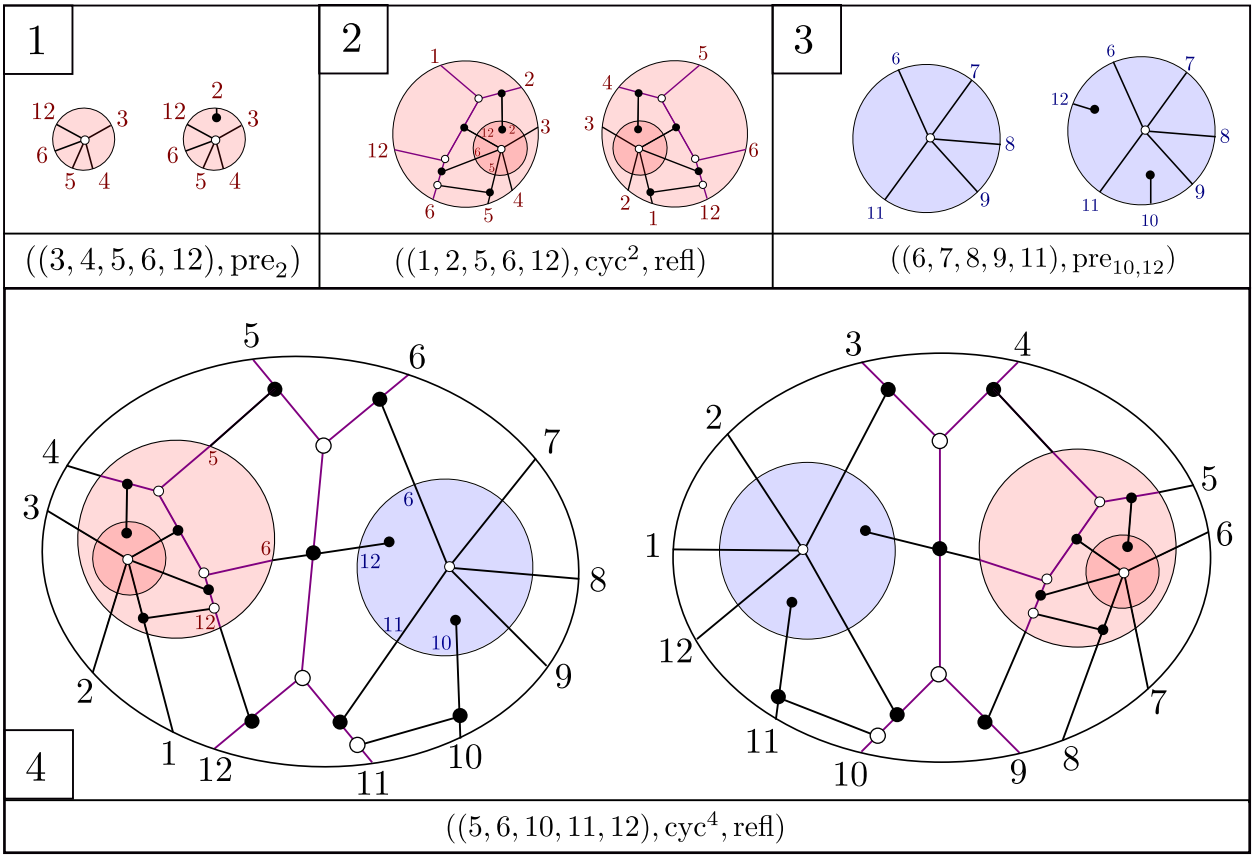

FIGURE 6. Illustration of building up a BCFW cell using the recipe $\mathfrak{r}$ of Example 2.27. Box i shows the result after the first i step-tuples. The result of the step $(a_i, b_i, c_i, d_i, n_i)$ is shown on the left in each box, and the results of the steps $\mathrm{pre}_{I_i}, \mathrm{cyc}^{r_i}$ and refl^{s_i} are shown on the right.

Notation 2.30. Let $\mathfrak{r}$ be a recipe for a BCFW cell $S \in \mathrm{Gr}^{\geq 0}_{k,N}$. Let FStep denote the final step, which is either $(a_k, b_k, c_k, d_k, n_k), \mathrm{pre}_{I_k}, \mathrm{cyc}$ or refl. If FStep $\neq (a_k, b_k, c_k, d_k, n_k)$, then we let $\mathfrak{p}$ denote the recipe obtained by replacing FStep with the identity. Note that $S_{\mathfrak{p}}$ is again a BCFW cell. If FStep $= (a_k, b_k, c_k, d_k, n_k)$, let $\mathfrak{r}_L$ and $\mathfrak{r}_R$ denote the recipes on N_L and N_R as in Definition 2.26. Then $\mathfrak{r}_L, \mathfrak{r}_R$ are recipes for BCFW cells $S_L \subset \mathrm{Gr}^{\geq 0}_{k_L,N_L}$ and $S_R \subset \mathrm{Gr}^{\geq 0}_{k_R,N_R}$ and $S = S_L \bowtie S_R$. Note that to avoid clutter, we will usually use L, R as subscripts rather than writing $S_{\mathfrak{r}_L}, S_{\mathfrak{r}_R}$.

Remark 2.31. In contrast with the bijective correspondence between standard BCFW cells and chord diagrams, multiple recipes could give rise to the same general BCFW cell. Even the sets of 5 indices that are involved in the BCFW products are not uniquely determined by the resulting cell.

3. Background: cluster algebra and BCFW tiles

In this section we review some of the connections between BCFW tiles and the cluster algebra of the Grassmannian $\mathrm{Gr}_{4,n}$. See e.g. [ELP+23, Section 3] for a relevant review on cluster algebras.

3.1. **Product promotion.** A key ingredient for connecting BCFW tiles to cluster algebras is *product promotion* – a map which is the algebraic counterpart of the BCFW product.

Definition 3.1. Using Notation 2.10, *product promotion* is the homomorphism

$$\Psi_B = \Psi : \mathbb{C}(\widehat{\mathrm{Gr}}_{4,N_L}) \times \mathbb{C}(\widehat{\mathrm{Gr}}_{4,N_R}) \to \mathbb{C}(\widehat{\mathrm{Gr}}_{4,n}),$$

induced by the following substitution:

$$\text{on } \widehat{\mathrm{Gr}}_{4,N_L}\colon\ b \ \mapsto\ \frac{(ba)\cap(cdn)}{\langle a\,c\,d\,n\rangle},$$

$$\text{on } \widehat{\mathrm{Gr}}_{4,N_R}\colon\ n \ \mapsto\ \frac{(ba)\cap(cdn)}{\langle a\,b\,c\,d\rangle},\ d \ \mapsto\ \frac{(dc)\cap(abn)}{\langle a\,b\,c\,n\rangle}.$$

The vector $(ij)\cap(rsq) := v_i\langle j\,r\,s\,q\rangle - v_j\langle i\,r\,s\,q\rangle = -v_r\langle i\,j\,s\,q\rangle + v_s\langle i\,j\,r\,q\rangle - v_q\langle i\,j\,r\,s\rangle$ is in the intersection of the 2-plane and the 3-plane spanned by v_i, v_j and v_r, v_s, v_q, respectively.

Theorem 3.2 below says[7] that Ψ is a *quasi-homomorphism* from the cluster algebra[8] $\mathbb{C}[\widehat{\mathrm{Gr}}^{\circ}_{4,N_L}]\times\mathbb{C}[\widehat{\mathrm{Gr}}^{\circ}_{4,N_R}]$ to the cluster algebra $\mathbb{C}[\widehat{\mathrm{Gr}}^{\circ}_{4,n}]$. See [ELP$^+$23, Definition 3.23] or [Fra16, Definition 3.1, Proposition 3.2] for the definition of a quasi-homomorphism.

Theorem 3.2. [ELP$^+$23, Theorem 4.7] *Product promotion Ψ is a quasi-homomorphism of cluster algebras. In particular, Ψ maps a cluster variable (respectively, cluster) of $\mathbb{C}[\widehat{\mathrm{Gr}}^{\circ}_{4,N_L}]\times\mathbb{C}[\widehat{\mathrm{Gr}}^{\circ}_{4,N_R}]$, to a cluster variable (respectively, sub-cluster) of $\mathbb{C}[\widehat{\mathrm{Gr}}^{\circ}_{4,n}]$, up to multiplication by Laurent monomials in $\mathcal{T}' := \{\langle a\,b\,c\,n\rangle, \langle a\,b\,c\,d\rangle, \langle b\,c\,d\,n\rangle, \langle a\,c\,d\,n\rangle\}$.*

Remark 3.3. Definition 3.1 and Theorem 3.2 extend also to the degenerate cases, e.g. for $a = 1$ (*upper promotion*), where $\Psi : \mathbb{C}(\widehat{\mathrm{Gr}}_{4,N_R}) \to \mathbb{C}(\widehat{\mathrm{Gr}}_{4,n})$, see [ELP$^+$23, Section 4.3].

Definition 3.4. Let x be a cluster variable of $\mathbb{C}[\widehat{\mathrm{Gr}}^{\circ}_{4,N_L}]$ or $\mathbb{C}[\widehat{\mathrm{Gr}}^{\circ}_{4,N_R}]$. We define the *rescaled product promotion* $\overline{\Psi}(x)$ of x to be the cluster variable of $\mathrm{Gr}_{4,n}$ obtained from $\Psi(x)$ by removing[9] the Laurent monomial in $\mathcal{T}'$ (c.f. Theorem 3.2).

The fact that product promotion is a cluster quasi-homomorphism may be of independent interest in the study of the cluster structure on $\mathrm{Gr}_{4,n}$. Much of the work thus far on the cluster structure of the Grassmannian has focused on cluster variables which are polynomials in Plücker coordinates with low degree; by contrast, the cluster variables we obtain can have arbitrarily high degree in Plücker coordinates. We introduce the following notation:

$$\langle a\,b\,c\,|\,d\,e\,|\,f\,g\,h\rangle := \langle a\,b\,c\,(d\,e)\cap(f\,g\,h)\rangle = \langle a\,b\,c\,d\rangle\,\langle e\,f\,g\,h\rangle - \langle a\,b\,c\,e\rangle\,\langle d\,f\,g\,h\rangle. \tag{1}$$

More generally, we consider polynomials called *chain polynomials* of degree $s+1$ as follows (see [ELP$^+$23, Definition 2.5]):

$$\begin{aligned}&\langle a_0\,b_0\,c_0\,|\,d_{1,0}\,d_{1,1}\,|\,b_1\,c_1\,|\,d_{2,0}\,d_{2,1}\,|\,b_2\,c_2\,|\,\ldots\,|\,d_{s,0}\,d_{s,1}\,|\,b_s\,c_s\,a_s\rangle\\ &= \sum_{t\in\{0,1\}^s} (-1)^{t_1+\cdots+t_s}\,\langle a_0\,b_0\,c_0\,d_{1,t_1}\rangle\,\langle d_{1,1-t_1}\,b_1\,c_1\,d_{2,t_2}\rangle\,\langle d_{2,1-t_2}\,b_2\,c_2\,d_{3,t_3}\rangle\,\cdots\,\langle d_{s,1-t_s}\,b_s\,c_s\,a_s\rangle\end{aligned} \tag{2}$$

[7] We will sometime omit the dependence on the indices $B = \{a, b, c, d, n\}$ in Ψ (and $\overline{\Psi}$) for brevity.

[8] $\mathbb{C}[\widehat{\mathrm{Gr}}^{\circ}_{4,N_L}]\times\mathbb{C}[\widehat{\mathrm{Gr}}^{\circ}_{4,N_R}]$ is a cluster algebra where each seed is the disjoint union of a seed of each factor.

[9] If $x = \langle bcdn\rangle$, then $\overline{\Psi}(x) = \Psi(x) = x$.

Example 3.5. For N_L and N_R as in Example 2.16, the only Plücker which changes is: $\Psi(\langle 1\,2\,4\,7\rangle) = \langle 1\,2\,7|3\,4|5\,6\,7\rangle/\langle 3\,4\,6\,7\rangle$, and $\overline{\Psi}(\langle 1\,2\,4\,7\rangle) = \langle 1\,2\,7|3\,4|5\,6\,7\rangle$ which is a quadratic cluster variable in $\mathrm{Gr}_{4,7}$, e.g. obtained by mutating $\langle 2367\rangle$ in the rectangle seed $\Sigma_{4,7}$ (see [ELP+23, Definition 3.12]).

3.2. **Coordinate cluster variables.** Using rescaled product promotion and Definition 2.3, we associate to each recipe $\mathfrak{r}$ a collection of compatible cluster variables $\mathbf{x}(\mathfrak{r})$ for $\mathrm{Gr}_{4,n}$. This will allow us to describe each (open) tile as the subset of the Grassmannian $\mathrm{Gr}_{k,k+4}$ where these cluster variables take on particular signs.

Definition 3.6 (Coordinate cluster variables of BCFW cells)**.** Let $S_{\mathfrak{r}} \subset \mathrm{Gr}_{k,n}^{\geq 0}$ be a BCFW cell. We use Notation 2.30. The *coordinate cluster variables* $\mathbf{x}(\mathfrak{r}) := \{\bar{\zeta}_i^{\mathfrak{r}}\}$ for $S_{\mathfrak{r}}$ are defined recursively as follows:

- If FStep $= (a, b, c, d, n) =: B$, then we define

$$\bar{\alpha}_k^{\mathfrak{r}} := \langle b\,c\,d\,n\rangle, \quad \bar{\beta}_k^{\mathfrak{r}} := \langle a\,c\,d\,n\rangle, \quad \bar{\gamma}_k^{\mathfrak{r}} := \langle a\,b\,d\,n\rangle, \quad \bar{\delta}_k^{\mathfrak{r}} := \langle a\,b\,c\,n\rangle, \quad \bar{\varepsilon}_k^{\mathfrak{r}} := \langle a\,b\,c\,d\rangle$$

$$\text{and for } i \neq k, \quad \bar{\zeta}_i^{\mathfrak{r}} := \begin{cases} \overline{\Psi}_B(\bar{\zeta}_i^L) \\ \overline{\Psi}_B(\bar{\zeta}_i^R) \end{cases} \text{ if the } i\text{th step-tuple is in } \begin{cases} \mathfrak{r}_L \\ \mathfrak{r}_R \end{cases}.$$

- If FStep $= \begin{cases} \text{refl} \\ \text{cyc} \\ \text{pre}_{I_k} \end{cases}$ then $\bar{\zeta}_i^{\mathfrak{r}} := \begin{cases} \text{refl}^*\,\bar{\zeta}_i^{\mathfrak{p}} \\ \text{cyc}^{-*}\,\bar{\zeta}_i^{\mathfrak{p}} \\ \bar{\zeta}_i^{\mathfrak{p}} \end{cases}$.

Note that $\mathbf{x}(\mathfrak{r})$ depends on the recipe $\mathfrak{r}$ rather than just the BCFW cell.

Notation 3.7. Given a cluster variable x in $\mathrm{Gr}_{4,n}$, we will denote by $x(Y)$ the functionary on $\mathrm{Gr}_{k,k+4}$ obtained by identifying Plücker coordinates $\langle I\rangle$ in $\mathrm{Gr}_{4,n}$ with twistor coordinates $\langle\langle I\rangle\rangle$ in $\mathrm{Gr}_{k,k+4}$ (cf. Definition 2.8).

Interpreting each cluster variable as a functionary, we describe each BCFW tile as the semialgebraic subset of $\mathrm{Gr}_{k,k+4}$ where the coordinate cluster variables take on particular signs. This appears as Corollary 7.12 in [ELP+23]:

Theorem 3.8 (Sign description for general BCFW tiles)**.** *Let $Z_{\mathfrak{r}}$ be a general BCFW tile. For each element x of $\mathbf{x}(\mathfrak{r})$, the functionary $x(Y)$ has a definite sign s_x on $Z_{\mathfrak{r}}^\circ$ and*

$$Z_{\mathfrak{r}}^\circ = \{Y \in \mathrm{Gr}_{k,k+4} : s_x\, x(Y) > 0 \text{ for all } x \in \mathbf{x}(\mathfrak{r})\}.$$

Example 3.9 (Coordinate cluster variables)**.** The coordinate cluster variables for $S_{\mathfrak{r}}$ in Figure 6 are obtained by applying the recursion in Definition 3.6:

i	$\bar{\alpha}_i$	$\bar{\beta}_i$	$\bar{\gamma}_i$	$\bar{\delta}_i$	$\bar{\varepsilon}_i$
1	$\langle 7\,8\,9\,\vert\,4\,3\,\vert\,9\,A\,B\rangle$	$\langle 6\,8\,9\,\vert\,4\,3\,\vert\,9\,A\,B\rangle$	$\langle 9\,A\,B\,\vert\,3\,4\,\vert\,6\,7\,\vert\,8\,9\,\vert\,3\,4\,5\rangle$	$\langle 6\,7\,8\,\vert\,4\,5\,\vert\,8\,9\,\vert\,3\,4\,\vert\,9\,A\,B\rangle$	$\langle 6\,7\,8\,9\rangle$
2	$\langle 5\,8\,9\,\vert\,4\,3\,\vert\,9\,A\,B\rangle$	$\langle 3\,4\,8\,9\rangle$	$\langle 3\,4\,5\,9\rangle$	$\langle 3\,4\,5\,8\rangle$	$\langle 4\,5\,8\,9\rangle$
3	$\langle 1\,2\,C\,\vert\,B\,A\,\vert\,3\,4\,9\rangle$	$\langle 1\,3\,C\,\vert\,A\,B\,\vert\,3\,4\,9\rangle$	$\langle 2\,3\,C\,\vert\,A\,B\,\vert\,3\,4\,9\rangle$	$\langle 1\,2\,3\,\vert\,B\,A\,\vert\,3\,4\,9\rangle$	$\langle 1\,2\,3\,C\rangle$
4	$\langle 3\,9\,A\,B\rangle$	$\langle 4\,9\,A\,B\rangle$	$\langle 3\,4\,9\,A\rangle$	$\langle 3\,4\,9\,B\rangle$	$\langle 3\,4\,A\,B\rangle$

See [ELP+23, Example 7.4] for more details.

3.3. **BCFW tiles.** In [ELP+23, Section 7] we proved that BCFW cells give tiles of the amplituhedron $\mathcal{A}_{n,k,4}(Z)$ by explaining how to invert the amplituhedron map $\tilde{Z}$ on the image $Z_{\mathfrak{r}}^{\circ} = \tilde{Z}(S_{\mathfrak{r}})$ of each BCFW cell $S_{\mathfrak{r}}$. For each point $Y \in Z_{\mathfrak{r}}^{\circ}$, the pre-image $\tilde{Z}^{-1}(Y)$ is a point in $\mathrm{Gr}_{k,n}^{\geq 0}$ represented by the *twistor matrix* $M_{\mathfrak{r}}^{\mathrm{tw}}(Y)$, whose entries are expressed in terms of ratios of the *coordinate functionaries* $\{\zeta_i^{\mathfrak{r}}(Y)\}_{i=1}^{5k}$ of $S_{\mathfrak{r}}$, see [ELP+23, Definition 7.1]. The coordinate functionaries are defined recursively in a similar way as in Definition 3.6 using product promotion. Moreover, they can be used to give a semilagebraic description of the tile. This is summarized in the theorem below, which appears as [ELP+23, Theorem 7.7].

Theorem 3.10 (General BCFW cells give tiles)**.** *Let $S_{\mathfrak{r}}$ be a general BCFW cell with recipe $\mathfrak{r}$. Then for all $Z \in \mathrm{Mat}_{n,k+4}^{>0}$, $\tilde{Z}$ is injective on $S_{\mathfrak{r}}$ and thus $Z_{\mathfrak{r}}$ is a tile. In particular, given $Y \in \tilde{Z}(S_{\mathfrak{r}})$, the unique preimage of Y in $S_{\mathfrak{r}}$ is given by (the rowspan of) of the twistor matrix $M_{\mathfrak{r}}^{\mathrm{tw}}(Y)$. Moreover,*

$$Z_{\mathfrak{r}}^{\circ} = \{Y \in \mathrm{Gr}_{k,k+4} : \zeta_i^{\mathfrak{r}}(Y) > 0 \text{ for all coordinate functionaries of } S_{\mathfrak{r}}\}.$$

For functionaries, we can introduce a similar notation as for the chain polyonmials in Equation (1):

$$\langle\!\langle a\,b\,c\,|\,d\,e\,|\,f\,g\,h\rangle\!\rangle \;=\; \langle\!\langle a\,b\,c\,d\rangle\!\rangle\,\langle\!\langle e\,f\,g\,h\rangle\!\rangle - \langle\!\langle a\,b\,c\,e\rangle\!\rangle\,\langle\!\langle d\,f\,g\,h\rangle\!\rangle. \tag{3}$$

More generally, we define *chain functionaries* of degree $s+1$ to be the polynomials obtained from Equation (2) by replacing Plücker coordinates $\langle I\rangle$ by twistor coordinates $\langle\!\langle I\rangle\!\rangle$. See [ELP+23, Definition 2.19].

Example 3.11 (Coordinate functionaries)**.** The coordinate functionaries for $S_{\mathfrak{r}}$ in Figure 6 are:

i	$\alpha_i(Y)$	$\beta_i(Y)$	$\gamma_i(Y)$	$\delta_i(Y)$	$\epsilon_i(Y)$
1	$\frac{\langle\!\langle 7\,8\,9\,\vert\,4\,3\,\vert\,9\,A\,B\rangle\!\rangle}{\langle\!\langle 3\,4\,9\,A\rangle\!\rangle}$	$-\frac{\langle\!\langle 6\,8\,9\,\vert\,4\,3\,\vert\,9\,A\,B\rangle\!\rangle}{\langle\!\langle 4\,9\,A\,B\rangle\!\rangle}$	$\frac{\langle\!\langle 9\,A\,B\,\vert\,3\,4\,\vert\,6\,7\,\vert\,8\,9\,\vert\,3\,4\,5\rangle\!\rangle}{\langle\!\langle 3\,4\,5\,8\rangle\!\rangle\langle\!\langle 4\,9\,A\,B\rangle\!\rangle}$	$-\frac{\langle\!\langle 6\,7\,8\,\vert\,4\,5\,\vert\,8\,9\,\vert\,3\,4\,\vert\,9\,A\,B\rangle\!\rangle}{\langle\!\langle 4\,5\,8\,9\rangle\!\rangle\langle\!\langle 4\,9\,A\,B\rangle\!\rangle}$	$\langle\!\langle 6\,7\,8\,9\rangle\!\rangle$
2	$-\frac{\langle\!\langle 5\,8\,9\,\vert\,4\,3\,\vert\,9\,A\,B\rangle\!\rangle}{\langle\!\langle 4\,9\,A\,B\rangle\!\rangle}$	$\langle\!\langle 3\,4\,8\,9\rangle\!\rangle$	$\langle\!\langle 3\,4\,5\,9\rangle\!\rangle$	$-\langle\!\langle 3\,4\,5\,8\rangle\!\rangle$	$\langle\!\langle 4\,5\,8\,9\rangle\!\rangle$
3	$-\frac{\langle\!\langle 1\,2\,C\,\vert\,B\,A\,\vert\,3\,4\,9\rangle\!\rangle}{\langle\!\langle 3\,4\,9\,B\rangle\!\rangle}$	$-\frac{\langle\!\langle 1\,3\,C\,\vert\,A\,B\,\vert\,3\,4\,9\rangle\!\rangle}{\langle\!\langle 3\,4\,9\,B\rangle\!\rangle}$	$\frac{\langle\!\langle 2\,3\,C\,\vert\,A\,B\,\vert\,3\,4\,9\rangle\!\rangle}{\langle\!\langle 3\,4\,9\,B\rangle\!\rangle}$	$-\frac{\langle\!\langle 1\,2\,3\,\vert\,B\,A\,\vert\,3\,4\,9\rangle\!\rangle}{\langle\!\langle 3\,4\,9\,B\rangle\!\rangle}$	$\langle\!\langle 1\,2\,3\,C\rangle\!\rangle$
4	$-\langle\!\langle 3\,9\,A\,B\rangle\!\rangle$	$\langle\!\langle 4\,9\,A\,B\rangle\!\rangle$	$\langle\!\langle 3\,4\,9\,A\rangle\!\rangle$	$-\langle\!\langle 3\,4\,9\,B\rangle\!\rangle$	$\langle\!\langle 3\,4\,A\,B\rangle\!\rangle$

See [ELP+23, Example 7.2] for more details.

For a standard BCFW tile Z_D, we call the coordinate cluster variables *domino cluster variables* or simply *domino variables*, and denote them as $\mathbf{x}(D) = \{\bar{\alpha}_i, \bar{\beta}_i, \bar{\gamma}_i, \bar{\delta}_i, \bar{\varepsilon}_i \mid 1 \leq i \leq k\}$. See [ELP+23, Theorem 8.4] for explicit formulas for the domino variables. The formulas have different cases depending on whether certain chords are head-to-tail siblings, same-end parent and child, or sticky parent and child (cf. terminology in Definition 2.19).

Example 3.12 (Domino cluster variables)**.** The domino cluster variables $\mathbf{x}(D)$ for the chord diagram D in Figure 3 are as follows. We will denote $(10, 11, 12, 13, 14, 15)$ as (A, B, C, D, E, F).

i	$\bar{\alpha}_i$	$\bar{\beta}_i$	$\bar{\gamma}_i$	$\bar{\delta}_i$	$\bar{\varepsilon}_i$
1	$\langle 4\,5\,6 \mid 2\,1 \mid 8\,9\,F\rangle$	$\langle 3\,5\,6 \mid 2\,1 \mid 8\,9\,F\rangle$	$\langle F\,8\,9 \mid 2\,1 \mid 3\,4 \mid 5\,6 \mid 8\,9\,F\rangle$	$\langle 3\,4\,5 \mid 2\,1 \mid 8\,9\,F\rangle$	$\langle 3\,4\,5\,6\rangle$
2	$\langle 6\,8\,9\,F\rangle$	$\langle 5\,8\,9\,F\rangle$	$\langle F\,1\,2 \mid 5\,6 \mid 8\,9\,F\rangle$	$\langle 5\,6\,8 \mid 2\,1 \mid 8\,9\,F\rangle$	$\langle 5\,6\,8\,9\rangle$
3	$\langle 2\,8\,9\,F\rangle$	$\langle 1\,8\,9\,F\rangle$	$\langle F\,1\,2 \mid 8\,9 \mid D\,E\,F\rangle$	$\langle 1\,2\,8\,F\rangle$	$\langle 1\,2\,8\,9\rangle$
4	$\langle B\,C\,D \mid 9\,8 \mid D\,E\,F\rangle$	$\bar{\beta}_4 = \bar{\alpha}_5$	$\langle 8\,9\,A\,B\rangle$	$\langle 9\,A\,B\,C\rangle$	$\langle A\,B\,C\,D\rangle$
5	$\langle A\,C\,D \mid 9\,8 \mid D\,E\,F\rangle$	$\langle 8\,9\,C\,D\rangle$	$\langle 8\,9\,A\,D\rangle$	$\langle 8\,9\,A\,C\rangle$	$\langle 9\,A\,C\,D\rangle$
6	$\langle 9\,D\,E\,F\rangle$	$\langle 8\,D\,E\,F\rangle$	$\langle 8\,9\,E\,F\rangle$	$\langle 8\,9\,D\,F\rangle$	$\langle 8\,9\,D\,E\rangle$

See [ELP+23, Example 8.5] for more details.

Definition 3.13 (Mutable and frozen domino variables)**.** Let $D \in \mathcal{CD}_{n,k}$ be a chord diagram, corresponding to a standard BCFW tile Z_D in $\mathcal{A}_{n,k,4}(Z)$. Let $\mathrm{Froz}(Z_D)$ denote the following collection of domino cluster variables:

- $\bar{\alpha}_i$ unless D_i has a sticky child
- $\bar{\beta}_i$ unless D_i starts where another chord ends or D_i has a same-end sticky parent.
- $\bar{\gamma}_i$ in all cases.
- $\bar{\delta}_i$ unless D_i has a same-end child.
- $\bar{\varepsilon}_i$ unless D_i has a same-end child.

Let $\mathrm{Mut}(Z_D)$ denote the complementary set of domino variables, i.e. $\mathrm{Mut}(Z_D) = \mathbf{x}(D) \setminus \mathrm{Froz}(Z_D)$.

Remark 3.14. One can show (see [ELP+23, Remark 8.2]) that if D_i has a same-end sticky parent D_p, then $\bar{\beta}_i = \bar{\alpha}_p$.

Example 3.15 (Mutable and frozen domino variables)**.** Let Z_D be the tile with the chord diagram D from Figure 3 and domino variables as in Example 3.12. Among those, the mutable variables are:

$$\bar{\alpha}_5,\ \bar{\alpha}_6,\ \bar{\beta}_2,\ \bar{\beta}_4,\ \bar{\beta}_6,\ \bar{\delta}_3,\ \bar{\delta}_5,\ \bar{\varepsilon}_3,\ \bar{\varepsilon}_5\ \in\ \mathrm{Mut}(Z_D).$$

Hence $\mathrm{Froz}(Z_D)$ consists of the remaining 21 domino variables. Note that $\bar{\alpha}_5 = \bar{\beta}_4$ by Remark 3.14.

Definition 3.16 (The seed Σ_D of a BCFW tile Z_D)**.** Let $D \in \mathcal{CD}_{n,k}$ be a chord diagram, and Z_D the corresponding BCFW tile. We define a seed $\Sigma_D = (\mathbf{x}(D), Q_D)$ as follows. The extended cluster $\mathbf{x}(D)$ has the sets $\mathrm{Mut}(Z_D)$ of mutable cluster variables and $\mathrm{Froz}(D)$ of frozen variables (recall Definition 3.13). To obtain the quiver Q_D, we consider each chord D_i in turn, check if it satisfies any of the conditions in the table below, and if so, we draw the corresponding arrows.

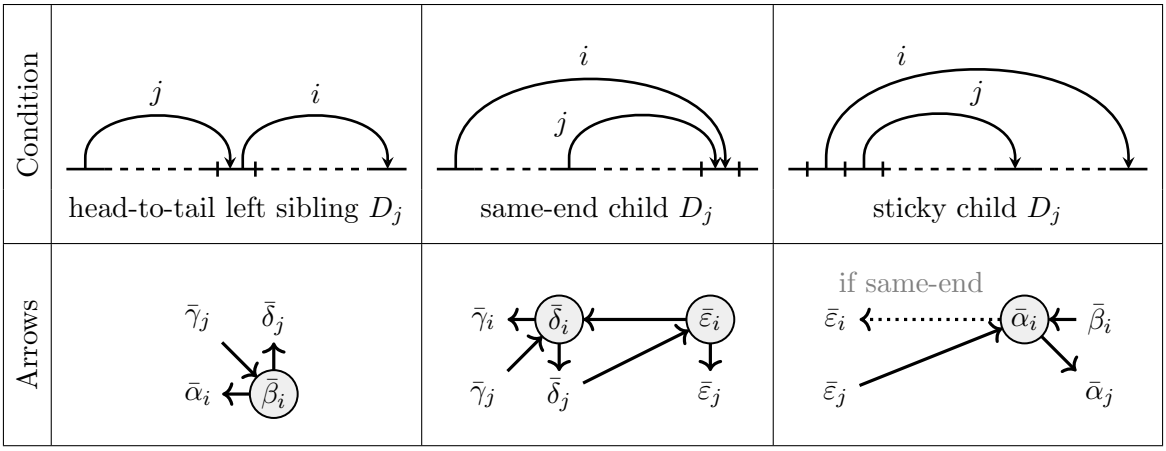

If D_i has sticky same-end child D_j then the dotted arrow from $\bar{\alpha}_i$ to $\bar{\varepsilon}_i$ appears, along with the usual arrows of the "sticky" and "same-end" cases. In view of Remark 3.14, in this case $\bar{\alpha}_i$ stands also for $\bar{\beta}_j$ as they are equal.

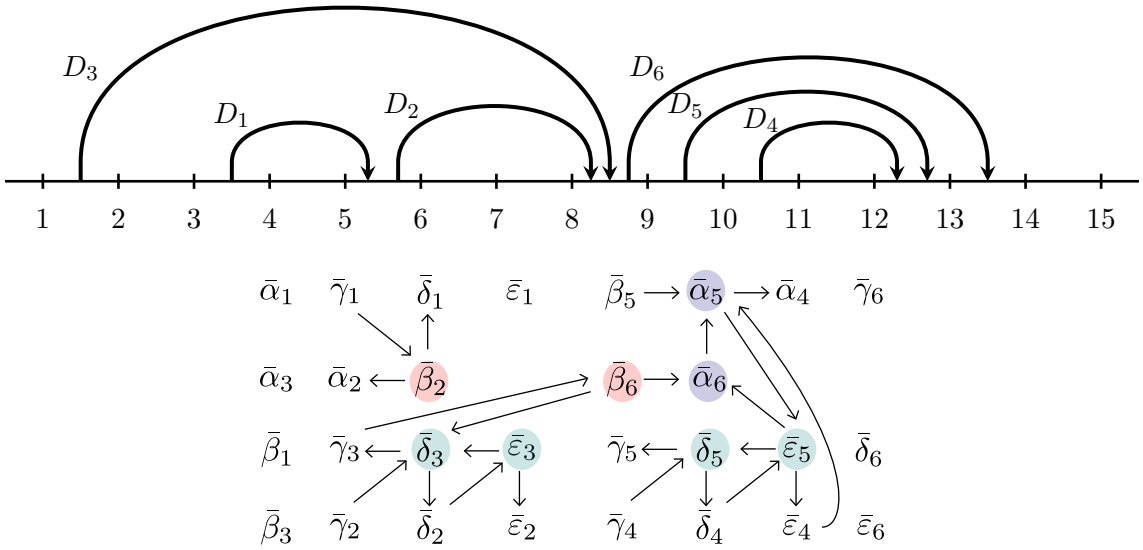

FIGURE 7. The seed Σ_D associated to the chord diagram D above (also in Figure 3). The variables $\mathbf{x}(D)$ are as in Example 3.12. The mutable variables $\mathrm{Mut}(Z_D)$ are circled; the other variables are the frozen variables $\mathrm{Froz}(Z_D)$. The colors (red, green, blue) indicate the different cases of Definition 3.16.

Example 3.17 (Seed of a standard BCFW tile)**.** The seed Σ_D from Figure 7 is built from Definition 3.16 by applying the rules for the following conditions. Head-to-tail left siblings: $(i,j) \in \{(2,1),(6,3)\}$; same-end child: $(i,j) \in \{(3,2),(5,4)\}$; sticky child: $(i,j) \in \{(6,5),(5,4)\}$.

Theorem 3.18 appears as Theorems 9.10 in [ELP+23].

Theorem 3.18 (The seed of a standard BCFW tile is a subseed of a $\mathrm{Gr}_{4,n}$ seed)**.** *Let $D \in \mathcal{CD}_{n,k}$. The seed $\Sigma_D = (\mathbf{x}(D), Q_D)$ is a subseed of a seed for $\mathrm{Gr}_{4,n}$. Hence every cluster variable (respectively, exchange relation) of $\mathcal{A}(\Sigma_D)$ is a cluster variable (resp., exchange relation) for $\mathrm{Gr}_{4,n}$.*

The following theorem characterizes the open BCFW tile Z_D° in terms of *any* extended cluster of $\mathcal{A}(\Sigma_D)$. It generalizes Theorem 3.8 for standard BCFW tiles and it appears as Theorem 9.11 in [ELP$^+$23].

Theorem 3.19 (Positivity tests for standard BCFW tiles)**.** *Let $D \in \mathcal{CD}_{n,k}$. Using Notation 3.7, every cluster and frozen variable x in $\mathcal{A}(\Sigma_D)$ is such that $x(Y)$ has a definite sign $s_x \in \{1, -1\}$ on the open BCFW tile Z_D°, and*

$$Z_D^\circ = \{Y \in \mathrm{Gr}_{k,k+4} : s_x \cdot x(Y) > 0 \text{ for all } x \text{ in any fixed extended cluster of } \mathcal{A}(\Sigma_D)\}. \tag{4}$$

The signs of the domino variables in Theorem 3.19 are given by [ELP$^+$23, Proposition 8.10].

Example 3.20 (Positivity test for a standard BCFW tiles)**.** For the tile Z_D with chord diagram D in Figure 7 and $\mathbf{x}(D)$ as in Example 3.12:

$$Z_D^\circ = \{Y \in \mathrm{Gr}_{6,10} : s_x \cdot x(Y) > 0 \text{ for all } x \in \mathbf{x}(D)\},$$

where the signs s_x are negative if x is among: $\bar{\alpha}_2$, $\bar{\alpha}_3$, $\bar{\alpha}_5 = \bar{\beta}_4$, $\bar{\beta}_1$, $\bar{\beta}_6$, $\bar{\gamma}_2$, $\bar{\delta}_1$, $\bar{\delta}_5$, $\bar{\delta}_6$. Otherwise, s_x is positive.

The following result appears as [ELP$^+$23, Theorem 7.16].

Theorem 3.21 (Cluster adjacency for general BCFW tiles)**.** *Let $Z_\mathfrak{r}$ be a general BCFW tile of $\mathcal{A}_{n,k,4}(Z)$. Each facet Z_S of $Z_\mathfrak{r}$ lies on a hypersurface cut out by a functionary $F_S(\langle\langle I \rangle\rangle)$ such that $F_S(\langle I \rangle) \in \mathbf{x}(\mathfrak{r})$. Thus $\{F_S(\langle I \rangle) : Z_S \text{ a facet of } Z_\mathfrak{r}\}$ consists of compatible cluster variables of $\mathrm{Gr}_{4,n}$.*

4. Facets of BCFW tiles

The main goal of this section is to prove Theorem 4.1, which characterizes the facets of standard BCFW tiles; this proof is in Section 4.1 and Section 4.2. Then in Section 4.3 we also state (without proof) a characterization of the facets of general BCFW tiles.

4.1. Facets of standard BCFW tiles.

Theorem 4.1 (Frozen variables as facets)**.** *Let $D \in \mathcal{CD}_{n,k}$ be a chord diagram, corresponding to a standard BCFW tile Z_D in $\mathcal{A}_{n,k,4}(Z)$. Then for each cluster variable $\bar{\zeta}_i \in \mathrm{Froz}(Z_D)$ (cf. Definition 3.13) there is a unique facet of Z_D which lies in the zero locus of the functionary $\bar{\zeta}_i(Y)$; the plabic graph of this facet is constructed in Theorem 4.11. Moreover, for any Z, there are no other facets of Z_D.*

We need several lemmas in order to prove Theorem 4.1. The first two are consequences of the Cauchy-Binet formula for the twistors (see, e.g., [ELP$^+$23, Lemma 2.16]). We recall the notion of *coindependence* ([ELP$^+$23, Definition 5.5])

Definition 4.2. Let $V \in \mathrm{Gr}_{k,n}^{\geq 0}$. A subset $I \subseteq [n]$ is *coindependent for V* if V has a nonzero Plücker coordinate $\langle J \rangle_V$, such that $J \cap I = \emptyset$. If $k = 0$ we declare all subsets to be coindependent. If S is a positroid cell in $\mathrm{Gr}_{k,n}^{\geq 0}$, then J is *coindependent for S* if J is coindependent for the elements of S.

Lemma 4.3. *Let $I = \{i_1, \ldots, i_m\} \in \binom{[n]}{m}$. If $\langle\langle CZ, Z_{i_1}, \ldots, Z_{i_m}\rangle\rangle \neq 0$, then I must be coindependent for $C \in \mathrm{Gr}^{\geq 0}_{k,n}$.*

Proof. If $\langle\langle CZ, Z_{i_1}, \ldots, Z_{i_m}\rangle\rangle \neq 0$, then by the second equation of [ELP$^+$23, Lemma 2.16], there must be some J such that $\langle J\rangle_C \neq 0$ and $J \cap I = \emptyset$. This means that I is coindependent for C. □

Definition 4.4 ([ELP$^+$23, Definition 11.1])**.** We say that functionary F has a *strong sign* on a positroid cell S if there exists an expansion of $F(\tilde{Z}(C))$, for $C \in S$, as a sum of monomials in the Plücker coordinates of C and the minor determinants of Z all of whose coefficients have the same sign.

Lemma 4.5. *Let $I \in \binom{[n]}{4}$, and let S be a cell of $\mathrm{Gr}^{\geq 0}_{k,n}$. Suppose that $\langle\langle I\rangle\rangle$ has a strong sign on Z°_S, but for some cell $S' \subset \overline{S}$, we have $\langle\langle I\rangle\rangle = 0$ on $Z_{S'}$. Then for each $J \in \binom{[n]}{k}$ disjoint from I, we must have $\langle J\rangle_C = 0$ for all $C \in S'$. In other words, I is not coindependent for S'.*

Proof. Since $\langle\langle I\rangle\rangle$ has a strong sign on Z_S, all nonzero terms of [ELP$^+$23, Lemma 2.16], which necessarily come from J for which J and I are disjoint, must have the same sign. Since $\langle\langle I\rangle\rangle = 0$ on $Z_{S'}$, all the above nonzero terms must vanish when we go to the cell S' in the boundary of S. But this means that all Plücker coordinates $\langle J\rangle$, with J disjoint from I, must vanish on S'. □

Lemma 4.6. *Let $S_L \subset \mathrm{Gr}^{\geq 0}_{k_L,N_L}$ and $S_R \subset \mathrm{Gr}^{\geq 0}_{k_R,N_R}$ be positroid cells, with plabic graphs G_L and G_R. Let $G = G_L \bowtie G_R$. If $\{a, b, n\}$ fails to be coindependent for S_L or $\{b, c, d, n\}$ fails to be coindependent for S_R, then for each $I \in \binom{\{a,b,c,d,n\}}{4}$, we have $\langle\langle I\rangle\rangle = 0$ on Z_G.*

Proof. We will prove the contrapositive. Suppose that for some $I \in \binom{\{a,b,c,d,n\}}{4}$, we have $\langle\langle I\rangle\rangle \neq 0$ on Z_{S_G}. Then by Lemma 4.3, I must be coindependent for the cell S_G. Then by [ELP$^+$23, Remark 5.6], the plabic graph G must have a perfect orientation $\mathcal{O}$ where all boundary vertices in I are sinks. But now it is a simple exercise to check that if in the graph $G_L \bowtie G_R$ which appears in Figure 8 (ignoring the arrows) we put sinks at the (outer) boundary vertices I, then there is a *unique* way to complete this to a perfect orientation of the "butterfly" portion of the graph. And in particular, this orientation will include the directed edges shown in Figure 8. But then the perfect orientation $\mathcal{O}$, restricted to G_L and G_R, must have sinks at vertices a, b, n of G_L, and at vertices b, c, d, n of G_R. But then $\{a, b, n\}$ and $\{b, c, d, n\}$ must be coindependent for S_L and S_R, respectively. □

Lemma 4.7. *For every cell $S \subseteq \partial S_D$ in the boundary of a standard BCFW cell S_D,*

$$Z_S \subseteq \partial Z_D.$$

So Z°_D is the interior of Z_D and $\partial Z^\circ_D = \partial Z_D = \tilde{Z}(\partial S_D)$.

Proof. The second and third statements follows from the first, using [ELP$^+$23, Corollary 11.17].

We now focus on proving the first statement. It is enough to prove it for facets, since images of boundary cells of higher codimensions are contained in the closure of the images of facets. By [ELT21, Proposition 7.10], each facet S of S_D is either a facet of another BCFW cell $S_{D'}$ or its image Z_S lies in the zero locus of a twistor coordinate $\langle\langle i, i+1, j, j+1\rangle\rangle$ for some i, j.

In the former case it follows that for every $p \in Z^\circ_S$, every open neighborhood of p intersects both Z°_D and $Z^\circ_{D'}$. By [ELT21, Theorem 1.4], which shows that the images of different standard

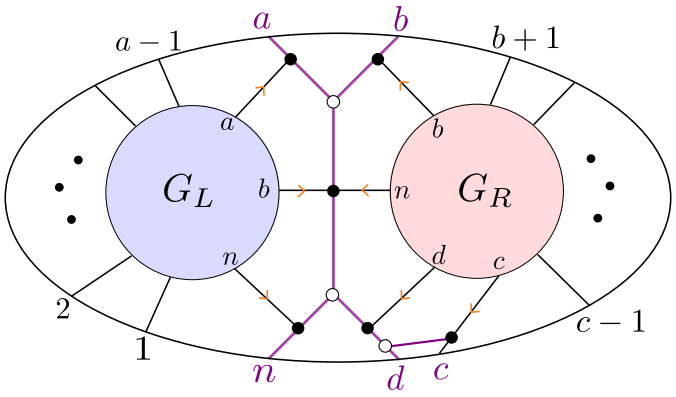

FIGURE 8.

BCFW cells do not intersect, we have that $Z_D^\circ \cap Z_{D'}^\circ = \emptyset$. Therefore Z_S° is indeed in the topological boundary of Z_D.

For the latter case, [ELT21, Proposition 8.1] shows that the intersection of the hypersurface $\{\langle\langle i, i+1, j, j+1\rangle\rangle = 0\}$ with $\mathcal{A}_{n,k,4}(Z)$ is contained in the topological boundary $\partial\mathcal{A}_{n,k,4}(Z)$. Hence if Z_S lies on this hypersurface, Z_S must also be contained in the topological boundary of Z_D. □

Lemma 4.8. *Let D be a standard BCFW cell, and let $\xi_1, \xi_2 \in \mathbf{x}(D)$ be two different domino cluster variables for Z_D. Then the intersection of zero loci of $\xi_1(Y), \xi_2(Y)$ (the natural identification between functionaries and homogenous polynomials in Plücker coordinates is explained in* [ELP$^+$23, Notation 7.11]*) meets Z_D in codimension greater than* 1*. It follows that for each mutable cluster variable $\xi \in \mathrm{Mut}(D)$, the zero locus of $\xi(Y)$ intersects Z_D in codimension greater than one.*

The proof of Lemma 4.8 is postponed to the next subsection.

Theorem 4.9. *Let $S = S_L \bowtie S_R$ be a BCFW cell, and suppose $I \in \binom{\{a,b,c,d,n\}}{4}$. Then there is at most one facet S' of S, such that among the five twistor coordinates coming from $\binom{\{a,b,c,d,n\}}{4}$, only $\langle\langle I\rangle\rangle$ vanishes on $Z_{S'}$. To construct the potential facet, we start from the graph in Figure 9 and remove the edge labeled by x_{12} (respectively, x_{10}, x_6, x_8, x_1), obtaining a graph $G^{(i)}$ corresponding to a cell $S^{(i)}$ (for $1 \le i \le 5$) such that $\langle\langle abcd\rangle\rangle$ (respectively, $\langle\langle abdn\rangle\rangle$, $\langle\langle bcdn\rangle\rangle$, $\langle\langle acdn\rangle\rangle$, $\langle\langle abcn\rangle\rangle$) is the unique twistor coordinate coming from $\binom{\{a,b,c,d,n\}}{4}$ which vanishes on $\tilde{Z}(S^{(i)})$. Moreover, we can realize the elements of $S^{(1)}$ using path matrices which have a row whose support is precisely $\{a, b, c, d\}$ (and similarly for the other $S^{(i)}$). If $G^{(i)}$ is reduced, then $S^{(i)}$ is the desired facet S'.*

Proof. Let G_L and G_R be reduced plabic graphs corresponding to S_L and S_R. By [Pos06, Theorem 18.5] (see also [ELP$^+$23, Theorem B.14]), any cell S' of codimension 1 in $\overline{S}$ comes from a plabic graph G' obtained by removing an edge e from $G_L \bowtie G_R$. Such an edge could be in G_L or G_R or in the "butterfly." Choose I from $\binom{\{a,b,c,d,n\}}{4}$. We first claim that if $\langle\langle I\rangle\rangle$ is the unique twistor coordinate among $\binom{\{a,b,c,d,n\}}{4}$ which vanishes on $Z_{S'}$, then edge e must come from the butterfly.

Suppose e does not come from the butterfly. Then $G' = G'_L \bowtie G'_R$, where either $G'_L = G_L$ and G'_R is obtained from G_R by removing an edge e, or vice versa. Since we are assuming the twistor coordinates from $\binom{\{a,b,c,d,n\}}{4}$ which are not $\langle\langle I\rangle\rangle$ do not vanish on $Z_{S'}$, Lemma 4.6 implies that $\{a, b, n\}$ is coindependent for the cell of G'_L, and $\{b, c, d, n\}$ is coindependent for the cell of

G'_R. Hence G'_L and G'_R have perfect orientations where $\{a, b, n\}$ and $\{b, c, d, n\}$ are sinks. But now by [ELP$^+$23, Lemma 10.4], all elements of $\binom{\{a,b,c,d,n\}}{4}$ are coindependent for S', the cell associated to $G'_L \bowtie G'_R$. Meanwhile we know by [ELP$^+$23, Lemma 11.6] that $\langle\langle I \rangle\rangle$ has a strong sign on Z_S. Therefore by Lemma 4.5, I is *not* coindependent for S'. This is a contradiction.

Now we know that if $\langle\langle I \rangle\rangle$ is the unique twistor coordinate among $\binom{\{a,b,c,d,n\}}{4}$ which vanishes on $Z_{S'}$, then S' has a plabic graph which is obtained from $G_L \bowtie G_R$ by removing an edge e from the butterfly. Let us choose perfect orientations of G_L and G_R where $\{a, b, n\}$ and $\{b, c, d, n\}$ are sinks. We can then complete this to a perfect orientation of $G = G_L \bowtie G_R$ with a source at d, as in Figure 9.

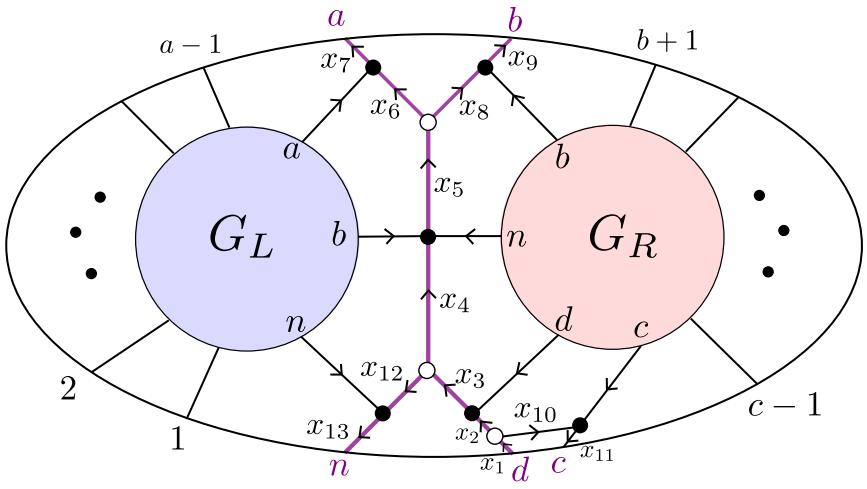

FIGURE 9. A perfect orientation of the butterfly, and the nonzero entries of row d in the associated path matrix.

Then the path matrix C associated to this perfect orientation has a row indexed by d with exactly five nonzero entries in positions a, b, c, d, n. If we weight the edges of G as in Figure 9, the row d of the path matrix is exactly as shown in the bottom of Figure 9.

Now notice that if we delete the edge e labeled by x_{12}, i.e. if $x_{12} = 0$, then our perfect orientation restricts to a perfect orientation of the remaining subgraph, and when we construct the path matrix C', row d will have support $\{a, b, c, d\}$. Thus the path matrix C', representing points of a cell $S^{(1)}$, will fail to be coindependent at $\{a, b, c, d\}$ and hence the twistor coordinate $\langle\langle a, b, c, d \rangle\rangle$ will vanish on $Z_{S^{(1)}}$. However, we can still find perfect orientations of the "butterfly $\backslash\{e\}$" with sinks at the other four elements of $\binom{\{a,b,c,d,n\}}{4}$, which all include n. So these other four twistor coordinates will not vanish on $Z_{S^{(1)}}$.

Similarly, if we delete the edge e labeled by x_{10}, then row d will have support $\{a, b, d, n\}$, and the analogous argument shows that the associated cell $S^{(2)}$ will fail to be coindependent at $\{a, b, d, n\}$. Moreover $\langle\langle a, b, d, n \rangle\rangle$ will be the unique twistor among $\binom{\{a,b,c,d,n\}}{4}$ which vanishes on $Z_{S^{(2)}}$. Meanwhile, if we delete the edge e labeled by x_6 (respectively, x_8), we get a cell $S^{(3)}$

(respectively, $S^{(4)}$) for which $\langle\langle b,c,d,n\rangle\rangle$ (respectively, $\langle\langle a,c,d,n\rangle\rangle$) is the unique twistor among $\binom{\{a,b,c,d,n\}}{4}$ which vanishes on the image of the cell under $\tilde{Z}$.

In order to discuss what happens when we delete the edge labeled by x_1, we first need to construct a new perfect orientation $\mathcal{O}'$, by reversing the directed path from d to n. Then when we delete the edge labeled by x_1, $\mathcal{O}'$ restricts to a perfect orientation, and the associated path matrix has a row indexed by n whose support is $\{a,b,c,n\}$. As before $\langle\langle a,b,c,n\rangle\rangle$ will be the unique twistor among $\binom{\{a,b,c,d,n\}}{4}$ which vanishes on $Z_{S^{(5)}}$.

This constructs the plabic graphs $G^{(i)}$ corresponding to the cells $S^{(i)}$ (for $1 \leq i \leq 5$) whose existence the theorem predicts. If $G^{(i)}$ is reduced, then $S^{(i)}$ is a facet of S, as desired.

To show that no other cells have the desired properties, we show that if we delete any other edge of the butterfly, we get a cell S' such that at least two twistors coordinates among $\binom{\{a,b,c,d,n\}}{4}$ vanish on $Z_{S'}$. For example if we delete the edges labeled x_2 or x_4, we still have a perfect orientation but now row d of the path matrix C' has support at most three, which means that at least two twistor coordinates among $\binom{\{a,b,c,d,n\}}{4}$ will vanish on $C'Z$. To analyze what happens if we delete any of the other edges we have to change the perfect orientation, but in all cases our path matrix C' will have a row whose support is a 1, 2, or 3-element subset of $\{a,b,c,d,n\}$, which means that at least two twistor coordinates among $\binom{\{a,b,c,d,n\}}{4}$ will vanish on $C'Z$. □

Lemma 4.10. *Let S be a standard BCFW cell, and let π be its trip permutation. Then $\pi(n) \notin \{1, n-1, n-2\}$, and $\pi(1) \neq n-1$.*

Proof. This follows from the Le-diagram description of standard BCFW cells from [KWZ20, Definition 6.2], or the related $\oplus$-diagram description given in [ELT21, Definition 2.24]. □

Theorem 4.11 (Plabic graphs for potential facets of standard BCFW tile)**.** *Let $G = G_L \bowtie G_R$ be a reduced plabic graph for the standard BCFW cell $S = S_L \bowtie S_R$ associated to a chord diagram D with top chord D_k. Use the notation of Theorem 4.9 and Figure 9, and identify the labels of edges of G with the edges themselves.*

(α). If D_k does not have a sticky child, then $G \setminus \{x_6\}$ is reduced.[10]
(β). D_k does not start where another chord ends if and only if $G \setminus \{x_8\}$ is reduced.
(γ). The graph $G \setminus \{x_{10}\}$ is reduced.
(δ). D_k does not have a same-end child if and only if $G \setminus \{x_1\}$ is reduced.
(ϵ). D_k does not have a same-end child if and only if $G \setminus \{x_{12}\}$ is reduced.

Before proving the theorem, we recall a useful lemma.

Lemma 4.12. [Pos06, Lemma 18.9] *Let G be a reduced plabic graph with trip permutation π, let e be an edge of G, and let $T_1 : i \to \pi(i)$ and $T_2 : j \to \pi(j)$ be the two trips in G that pass through e (the trips will pass through this edge in two different directions). Then $G \setminus \{e\}$ is reduced if and only if the pair $(i, \pi(i))$ and $(j, \pi(j))$ is a simple crossing in π.*

Proof of Theorem 4.11. Case (α). If D_k does not have a sticky child, then G_R has a black lollipop at b. This means that in G, the edge connecting vertex b in G_R to the "butterfly" can be contracted. The trips going through edge x_6 are shown in Figure 10. Since these two trips end at adjacent

[10]The converse may not be true.

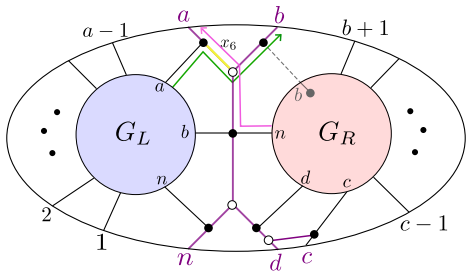

FIGURE 10. If D_k does not have a sticky child, then $G \setminus \{x_6\}$ is reduced.

boundary vertices, they must be part of a simple crossing. Therefore by [Pos06, Lemma 18.9], $G \setminus \{x_6\}$ is reduced.

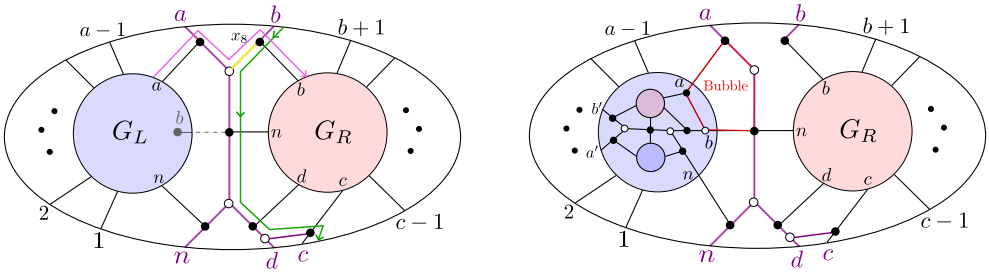

FIGURE 11. Left: if D_k does not start where another chord ends then $G \setminus \{x_8\}$ is reduced. Right: if D_k starts where another chord ends then $G \setminus \{x_8\}$ is non-reduced.

Case (β). Suppose that D_k does not start where another chord ends. Then G_L has a black lollipop at vertex b, which means that the edge (shown dashed in Figure 11) connecting that vertex to the butterfly can be contracted. The two trips which pass through x_8 are shown in pink and green in Figure 11. By Lemma 4.10, $\pi_{G_L}(n) \neq a$ and so the pink trip in G must start at the left part of the graph, i.e. at some element in $\{1, 2, \ldots, a-1\}$. We also claim that the pink trip in G must end at the right part of the graph, i.e. at some element in $\{b+1, b+2, \ldots, c-1\}$, otherwise the pink and green trips would have a *bad double crossing* and G would fail to be reduced [Pos06, Theorem 13.2]. But now it is clear that the pink and green trips must form a simple crossing, because there is no other trip in G that starts at an element of $\{1, 2, \ldots, a\}$ and ends at an element of $\{b+1, b+2, \ldots, c-1\}$. Therefore by [Pos06, Lemma 18.9], $G \setminus \{x_8\}$ is reduced.

Now suppose that D_k starts where another chord ends. Then G_L has the form shown at the right of Figure 11: in particular, the vertices a and b of G_L are connected by a black-white bridge. But then when we delete edge x_8, the resulting graph has a configuration of vertices which is move-equivalent to a bubble (cf [ELP+23, Definition B.2]), as shown in the right of Figure 11. Therefore $G \setminus \{x_8\}$ is not reduced.

Case (γ). The two trips passing through x_{10} are shown in Figure 12. Since these two trips end at c and d, there cannot be another trip ending between c and d, hence they represent a simple crossing. Therefore by Lemma 4.12, $G \setminus \{x_{10}\}$ is reduced.

Case (δ). Suppose that D_k does not have a same-end child. Then D does not have another chord ending at (c, d), and hence in G_R, the vertex d will be a black lollipop that can be contracted. First

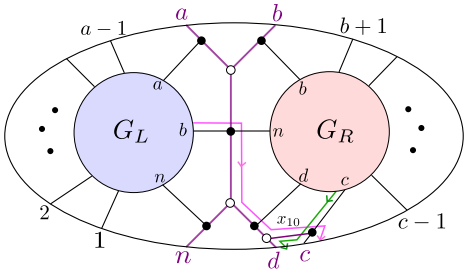

FIGURE 12. The graph $G \setminus \{x_{10}\}$ is reduced.

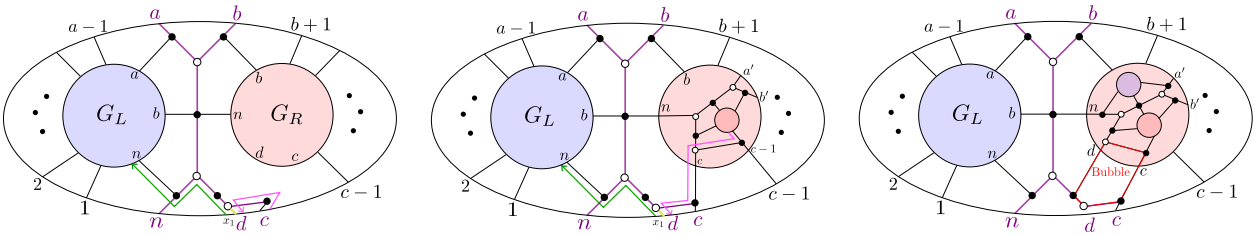

FIGURE 13. Left: If D_k does not have a same-end child and D has no chord ending at $(c-1,c)$, then $G \setminus \{x_1\}$ is reduced. Middle: If D_k does not have a same-end child and D does have a chord ending at $(c-1,c)$, then $G \setminus \{x_1\}$ is reduced. Right: if D_k has a same-end child then $G \setminus \{x_1\}$ is not reduced.

suppose there is no chord in D ending at $(c-1,c)$, then there is also a lollipop in G_R at c, and G looks as shown at the left of Figure 13. Then one of the trips through edge x_1 goes from c to d, so the two trips passing through x_1 must form a simple crossing. Therefore by [Pos06, Lemma 18.9], $G \setminus \{x_1\}$ is reduced. Now suppose there *is* a chord in D ending at $(c-1,c)$. Then G looks as shown in the middle of Figure 13. By Lemma 4.10, $\pi_{G_R}(1) \neq n-1$ and $\pi_{G_R}(n) \neq n-1$, so the pink trip must start at an element of $\{b+1,\dots,c-1\}$. Similarly, by Lemma 4.10, $\pi_{G_L}(n) \neq n-2$ and $\pi_{G_L}(n) \neq n-1$, so the green trip must end at an element of $\{1,2,\dots,a-1\}$. But now the pink and green trips must form a simple crossing, because there is no other trip that can start at an element of $\{b+1,\dots,c-1\}$ and end at an element of $\{1,2,\dots,a-1\}$. Therefore $G \setminus \{x_1\}$ is reduced.

Now suppose that D_k has a same-end child. Then G_R has a black-white bridge at vertices c,d, and when we delete $\{x_1\}$, $G \setminus \{x_1\}$ looks as in the right of Figure 13. We obtain a face which is move-equivalent to a bubble, so $G \setminus \{x_1\}$ is not reduced.

Case (ϵ). Suppose that D_k does not have a same-end child. Then G_R has a black lollipop (which can be contracted), and hence the two trips passing through x_{12} are as shown at the left of Figure 14. Since these two trips start at adjacent vertices d and n, they must form a simple crossing. Therefore by [Pos06, Lemma 18.9], $G \setminus \{x_{12}\}$ is reduced.

Now suppose that D_k does have a same-end child. Then G_R has a black-white bridge, as shown in the right of Figure 14. G_R is itself the plabic graph of a standard BCFW cell, so we can write it as $G_R = G_{L'} \bowtie G_{R'}$. If d is a black lollipop in $G_{R'}$, then we can contract the edge joining that lollipop to the butterfly in G_r, and then we find that region R_1 in Figure 14 is move-equivalent to a

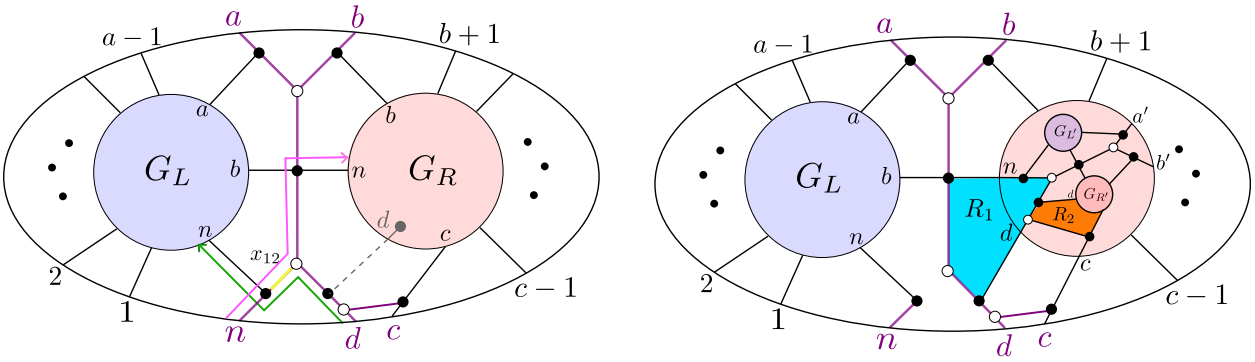

FIGURE 14. Left: if D_k does not have a same-end child then $G \setminus \{x_{12}\}$ is reduced. Right: if D_k has a same-end child then $G \setminus \{x_{12}\}$ is not reduced.

bubble. On the other hand, if d is not a black lollipop in $G_{R'}$, then D_k has a same-end grandchild, so $G_{R'}$ has a black-white bridge. Then one can do a square move at R_2 which turns R_1 into a bubble. Therefore $G \setminus \{x_{12}\}$ is not reduced. □

Proof of Theorem 4.1. By Lemma 4.7, all facets of S_D map to the boundary of Z_D, so any cell in ∂S_D whose image is codimension 1 in Z_D is a facet of Z_D. Theorem 3.21 shows that all facets of Z_D lie in the zero locus of a cluster variable in $\mathbf{x}(D)$. By Lemma 4.8, no facet is contained in the zero locus of a mutable cluster variable $\mathrm{Mut}(Z_D)$. Thus, we are left to show the following.

Claim 4.13. For each frozen variable $\bar{\zeta}$ in $\mathrm{Froz}(D)$, there is exactly one cell S of codimension 1 in $\overline{S}_D$ such that Z_S is codimension 1 in Z_D and Z_S lies in the zero locus of $\bar{\zeta}$.

In [ELT21, Section 7] it was shown that each facet S' of a standard BCFW cell S_D either:

(1) maps to the interior of $\mathcal{A}_{n,k,4}(Z)$, in which case it maps injectively [ELT21, Proposition 8.2], and lies in the zero locus of a coordinate functionary,[11] or
(2) maps to the boundary of $\mathcal{A}_{n,k,4}(Z)$, in which case $Z_{S'}$ lies in the zero locus of a domino cluster variable of the form $\langle\langle i, i+1, j, j+1\rangle\rangle$.

In the first case, Claim 4.13 follows from results of [ELT21], as we now explain. Those facets of S_D which map injectively to the interior of the amplituhedron are in bijection with the elements of $\mathrm{Froz}(Z_D)$ which do not have the form $\langle\langle i, i+1, j, j+1\rangle\rangle$, and can be explicitly constructed using the BCFW recursion, but with one parameter set to 0 [ELT21, Lemma 7.9]. Then using the arguments from the proof of Theorem 3.21 , one can see that if S' is a facet of S_D where a single BCFW coordinate ζ_i vanishes, then $Z_{S'}$ lies in the zero locus of the corresponding cluster variable $\bar{\zeta}_i$. Moreover, for every BCFW parameter, there is at most one facet of S_D where only that parameter vanishes (cf. [ELT21, Lemmas 7.9, 7.13, 7.14, 7.15]).

We now show that Claim 4.13 holds for frozen domino variables of the form $\langle i, i+1, j, j+1\rangle$, using results of [ELT21, Section 7] as well as Theorem 4.9 and Theorem 4.11. We use the notation of [ELT21] which are close to the ones used in this paper, but not identical.

[11] [ELT21, Section 7] is phrased using entries and 2-by-2 minors of the domino matrix, which are the same as our BCFW coordinates.

Step 1: constructing the facets. Since we are concerned only with facets of Z_D where a boundary twistor $\langle\langle i, i+1, j, j+1\rangle\rangle$ vanishes, we can use Theorem 4.9 and Theorem 4.11 to build the plabic graph G corresponding to the facet (we will show in Step 3 below that the image of the cell S_G has codimension 1 in Z_D). Concretely, in order to construct the graph G corresponding to the facet of Z_D where $\bar{\zeta}_i$ vanishes (where $\bar{\zeta}_i$ is a boundary twistor), we follow the procedure for constructing S_D, but at the ith step we remove the edge of the butterfly dictated by Theorem 4.9.

Step 2: Uniqueness of facets where a given cluster variable vanishes. We use induction to show that for each $\langle\langle i, i+1, j, j+1\rangle\rangle \in \mathrm{Froz}(Z_D)$, there is at most one facet of a tile Z_D in its zero locus. From [ELP+23, Lemma 10.5] , we know that each facet $Z_{S'}$ of a BCFW tile Z_D either (1) lies in the vanishing locus of a domino variable $\bar{\zeta}_k$ of the kth chord (which is a twistor coordinate with indices in $\{a, b, c, d, n\}$), or (2) the cell S' is the BCFW product of a BCFW cell and a facet of another BCFW cell. By induction, the tiles coming from Case (2) lie in the vanishing locus of distinct cluster variables; and these cluster variables must all be different from the twistor coordinates of the kth chord. (The only case when a coordinate cluster variable from S_L or S_R promotes to a twistor coordinate for the top chord is the case of $\bar{\beta}_i$ where D_i is a sticky same-end child of D_k; in this case, $\bar{\beta}_i = \bar{\alpha}_k = \langle\langle bcdn\rangle\rangle$ which is not a boundary twistor since D_k has a child.) In Case (1), Theorem 4.9 shows that there is at most one facet $Z_{S'}$ of Z_{S_D} which lies in the zero locus of a single chord twistor of the kth chord. But now by Lemma 4.8, if two cluster variables vanish on $Z_{S'}$, it must have codimension at least 2, so all facets of Z_D must lie in the vanishing locus of distinct cluster variables.

Step 3: Injectivity of the amplituhedron map. In light of Theorem 4.9, we can alternatively construct the facets by following the recipe of Definition 2.15 , but setting exactly one of the BCFW parameters $\{\alpha_i, \beta_i, \delta_i, \gamma_i, \epsilon_i\}$ for $1 \le i \le k$ equal to 0 at the appropriate BCFW step. Using slightly different conventions, such a construction[12] was given in [ELT21, Definition 7.6 and Lemma 7.7] for most facets, building each facet in terms of the operations $\mathrm{pre}_i, \mathrm{inc}_i, x_i(\mathbb{R}_+), y_i(\mathbb{R}_+)$.

Now we need to show that the amplituhedron map restricted to S', the facet of S obtained by setting a particular BCFW parameter $\star$ to 0, is injective. The proof is similar to the proof of [ELP+23, Theorem 7.7]. The positroid cell S' is constructed by a sequence of adding zero columns, BCFW products, and a single "degenerate" BCFW product.

As in the proof of [ELP+23, Theorem 7.7] the proof of injectivity follows by showing that injectivity persists through the different steps of the construction of S'. The treatment in the cases of adding a zero column, and doing a BCFW product is identical to the treatment in [ELP+23, Theorem 7.7] , relying on [ELP+23, Theorem 11.3] (as before we need to verify that $\{b_i, c_i, d_i, n\}$ is coindependent at the time of the ith BCFW step). The treatment in the single degenerate BCFW product is also completely analogous to that of[ELP+23, Theorem 7.7] , and this proves the injectivity.

Note, however, that in the application of [ELP+23, Lemma 11.13] for the degenerate step, the coordinate $\star$ turns out to be 0, while the other four keep the same sign they would have had on the BCFW cell at that stage. This twistor will be promoted, according to [ELP+23, Theorem 11.3] to a functionary vanishing on this facet. The same argument used in the proof of Theorem 3.21 shows that each facet lies in the zero locus of the corresponding *reduced* functionary. In light of the

[12]This construction was called the $(D, \star)-$*extended domino form* for $\star \in \{\alpha_i, \beta_i, \gamma_i, \delta_i, \varepsilon_i, \eta_{ij}, \theta_{ij}\}$.

uniqueness discussion above, we see that each such reduced boundary functionary corresponds to a unique facet. It also follows that the facet is characterized as the locus where the corresponding functionary vanishes, but the other coordinate functionaries keep their signs. Lemma 4.7 shows that the facets indeed map to the boundary of the tile.

□

Note that the uniqueness in the above proof follows from two facts. First, if a facet in the domain has image which is not a facet at some time of the cell construction process, then the BCFW product of this facet with a standard BCFW cell will also have image which is not a facet. Second, when a new facet in the domain (which corresponds to the rightmost top chord at a given time of the process) maps to a facet of the tile, it is the maximal face in the domain, among those which map into the zero locus of the corresponding chord twistor, hence other components in this zero locus are of lower dimension already in the domain.

4.2. **Proof of Lemma 4.8.** The proof of the lemma will use the notion of transversality. For this we recall some notions and facts.

Definition 4.14. Let X be an n dimensional manifold with an atlas $\{(U_\alpha, \phi_\alpha : U_\alpha \to \mathbb{R}^n)\}_{\alpha\in A}$. We say that a set $L \subseteq X$ *is of measure* 0*,* if for every $\alpha \in A$, the set $\phi_\alpha(L \cap U_\alpha)$ is of Lebesgue measure 0 in $\mathbb{R}^n$. If $M \subset X$ is the complement of a measure 0 subset, we say that *almost every* $x \in X$ *belongs to* M.

Definition 4.15. Let $f : X \to M$ be a smooth map between smooth manifolds X, M. Let L be a smooth submanifold of M. We say that f is *transverse* to L, and write $f \pitchfork L$ if for every $x \in f^{-1}(L)$

$$df_x(T_xX) + T_{f(x)}L = T_{f(x)}M,$$

where T_xX denotes the tangent space of X at $x \in X$, and df_x is the differential map at x, which maps T_xX into $T_{f(x)}M$.

Theorem 4.16 (Thom's Parametric Transversality Theorem)**.** *Let X be a smooth manifold, let B, M be smooth manifolds and let L be a submanifold of M. Let $f : X \times B \to M$ be a smooth map. Suppose that $f \pitchfork L$. Then for almost every $b \in B$ the map*

$$f(-, b) : X \times \{b\} \to M$$

is transverse to M.

We first prove a general "almost-every Z" result.

Lemma 4.17. *The zero locus in the amplituhedron $\mathcal{A}_{n,k,4}(Z)$ of two different irreducible functionaries (as in Definition 2.9) is of codimension at least* 2 *for almost all Z.*

We know from [GLS13, Theorem 1.3] that all cluster variables are irreducible; therefore, in light of Definition 2.9, functionaries which correspond to cluster variables of $\mathrm{Gr}_{4,n}$ are irreducible.

Proof. We will prove the lemma in the B-amplituhedron (cf. [KW19, Definition 3.8] (see also [ELP$^+$23, Definition 2.20]) $\mathcal{B}_{n,k,4}(W)$, where W is the column span of Z. This will imply the result for $\mathcal{A}_{n,k,4}(Z)$, since the map f_Z of [ELP$^+$23, Proposition 2.21] (which combines [KW19, Lemma

3.10 and Proposition 3.12]) is a diffeomorphism from a neighborhood of the B-amplituhedron to a neighborhood of $\mathcal{A}_{n,k,4}(Z)$. The map between the two spaces takes the zero locus of an irreducible functionary to the zero locus of an irreducible polynomial in the Plücker coordinates of $\mathrm{Gr}_{4,n}$, and we consider its intersection with $\mathcal{B}_{n,k,4}(W)$. It will be enough to show that its intersection with $\mathrm{Gr}_4(W)$, for a generic $W \in \mathrm{Gr}_{k+4,n}$ is of codimension 2. We will use Thom's transversality. Let $M = \mathrm{Gr}_{4,n}$, and L the intersection of zero loci of the two functions. Then L is of codimension 2. Let B be a small ball around $W \in \mathrm{Gr}_{k+4,n}$, and $X = \mathrm{Gr}_4(W)$. Identify the fiber bundle $F \to B$ whose fiber over $W' \in B$ is $\mathrm{Gr}_4(W')$ with $X \times B$. This can be done since the two spaces are diffeomorphic, for B small enough. The map $f : X \times B \to M$ is defined by

$$f(V, W') = V,$$

where $W' \in B,\ V \in \mathrm{Gr}_4(W')$ and in the right hand side V is considered as an element of $\mathrm{Gr}_{4,n}$. Clearly $df_{V,W'}(T_{V,W'}X \times B) = T_V \mathrm{Gr}_{4,n}$, so that the assumption of Theorem 4.16 is met. Thus, for almost every $W' \in B$, the intersection $\mathrm{Gr}_4(W') \cap L$ is of codimension 2, hence the intersection with L of the $B-$amplituhedron, for almost every W, is of codimension at least 2. □

Proof of Lemma 4.8. The last statement follows from the first one, since if ξ is a mutable variable for Z_D, then the mutation relation has the form

$$\xi\xi' = A + B,$$

where ξ is the variable of interest, and A, B are products of other cluster variables. Moreover, by [ELP$^+$23, Proposition 9.27], A, B have the same sign on Z_D°. Thus, the vanishing of ξ implies the vanishing of at least one more cluster variable.

Every facet of Z_D lies in the zero locus of a cluster variable, by Theorem 3.21. By [ELP$^+$23, Theorem 11.3] we know that the cluster variables of Z_D have a strongly positive expression, hence every such functionary either vanishes identically on a given boundary Z_S, for all positive Z, or never vanishes there, for all positive Z. Let $S_1, \ldots, S_N$ be the facets of S_D which map to the zero locus of a single cluster variable.

From the previous lemma it follows that for almost all positive Z the remaining faces of S_D map to the union of finitely many codimension 2 submanifolds of Z_D. These submanifolds are contained in ∂Z_D, using Lemma 4.7 and the fact that no cluster variable of Z_D vanishes on Z_D°.

Denote by $L(\xi_1, \xi_2) \subset Z_D$ the vanishing locus of ξ_1 and ξ_2 in Z_D. Let $S'_1, \ldots, S'_M$ be the faces of D which map to $L(\xi_1, \xi_2)$. Note that

$$L(\xi_1, \xi_2) \subseteq Z_D \setminus \left(Z_D^\circ \sqcup_{i=1}^N Z_{S_i}^\circ\right) \subseteq \partial Z_D. \tag{5}$$

For almost all positive Z, $L(\xi_1, \xi_2)$ is of codimension at least 2. We will now show that for almost all positive Z

$$L(\xi_1, \xi_2) \subseteq \sqcup_i Z_{S_i},$$

together with (5) this implies, that for almost all positive Z, and every $j = 1, \ldots, M$

$$Z_{S'_j} \subseteq \sqcup_{i=1}^N \sqcup_{S' \text{ is a face of } S_i} Z_{S'}, \tag{6}$$

that is, the union of images of faces of D of codimension at least 2.

In order to show (5), take an arbitrary $p \in L(\xi_1, \xi_2)$. We will show that every neighborhood U of p contains a point from $\bigcup_{i=1}^{N} Z^{\circ}_{S_i}$. Indeed, assume without loss of generality that U is connected, since p belongs to the boundary of Z_D, we can find two points $q_0 \in Z_D \cap U,\ q_1 \in U \setminus Z_D$. We can find a path $(q_t)_{t\in[0,1]} \subset U$ from q_0 to q_1 in U not passing throw the intersection of zero loci of any two different cluster variables, which we assume to be of codimension 2 or more (see, e.g., the proof of [ELT21, Proposition 8.5]). Let t be the last time where $q_t \in Z_D$. Then q_t must be in the zero locus of a single cluster variable, hence in some Z_{S_i}.

Now, since (6) holds for almost every positive Z, and both its left hand and right hand are images of compact sets, it holds in fact for every positive Z. Indeed, if Z is the limit of $(Z_i)_{i=1}^{\infty}$ where for each Z_i (6) holds, it also holds for Z.

□

4.3. **Facets of general BCFW tiles.** We now describe, without proof, the facets of general BCFW tiles in Claim 4.25. Instead of the recipe in Definition 2.26, it is convenient to use a slightly different indexing set for BCFW tiles.

Definition 4.18. Let $\mathfrak{r}$ be a recipe with k step-tuples, which is composed by a recipe $\mathfrak{r}_L$ followed by a recipe $\mathfrak{r}_R$ followed by a step-tuple $((a_k, b_k, c_k, d_k, n_k), \mathrm{pre}_{I_k}, \mathrm{cyc}^{r_k}, \mathrm{refl}^{s_k})$. We introduce the following collection of 5-tuples $\tilde{D} = \{(\tilde{a}_i, \tilde{b}_i, \tilde{c}_i, \tilde{d}_i, \tilde{n}_i)\}_{i=1}^{k} = \tilde{D}_L \cup \tilde{D}_R \cup \tilde{D}_k$ we call *generalized chords* defined recursively as:

- $\tilde{D}_k = (\tilde{a}_k, \tilde{b}_k, \tilde{c}_k, \tilde{d}_k, \tilde{n}_k) = \mathrm{refl}^{s_k} \circ \mathrm{cyc}^{r_k}(a_k, b_k, c_k, d_k, n_k)$,
- $\tilde{D}_L = \mathrm{refl}^{s_k} \circ \mathrm{cyc}^{r_k} \tilde{D}'_L$ and $\tilde{D}_R = \mathrm{refl}^{s_k} \circ \mathrm{cyc}^{r_k} \tilde{D}'_R$,

where $\tilde{D}'_L$ (resp. $\tilde{D}'_R$) are the generalized chords for the recipe $\mathfrak{r}_L$ (resp. $\mathfrak{r}_R$).

Notation 4.19. Given a BCFW cell $S_{\mathfrak{r}}$, we will sometime label it as $S_{\tilde{D}}$ in terms of the corresponding generalized chords $\tilde{D}$. We denote by $\tilde{D}_L^{(j)} \cup \tilde{D}_R^{(j)} \cup \tilde{D}_j$ the generalized chords of the recipe $\mathfrak{r}^{(j)}$ obtained from $\mathfrak{r}$ by performing only the first j step-tuples. Here $\tilde{D}_L^{(j)}$ (resp. $\tilde{D}_R^{(j)}$) are the generalized chords of $\mathfrak{r}_L^{(j)}$ (resp. $\mathfrak{r}_R^{(j)}$).

Example 4.20. Consider the BCFW cell $S_{\mathfrak{r}}$ of Figure 6. Its generalized chords are:
$\tilde{D} = \{(6, 7, 8, 9, 3), (4, 5, 8, 9, 3), (3, 2, 1, 12, 10), (4, 3, 11, 10, 9)\}$. Its plabic graph is as in Figure 15.

We introduce the definition of *condensability* and *condensations* of a BCFW cell $S_{\mathfrak{r}}$ as follows.

Definition 4.21. Let $S_{\tilde{D}} \subseteq \mathrm{Gr}^{\geq 0}_{k,n}$ be a BCFW cell, and $\tilde{D} = \{\tilde{D}_i\}_{i=1}^{k}$ the corresponding generalized chords. For $i \in [k]$, $\tilde{f}_i \in \{\tilde{a}_i, \tilde{b}_i, \tilde{c}_i, \tilde{d}_i, \tilde{n}_i\}$ we say that $S_{\tilde{D}}$ is $\tilde{f}_i$*-condensable* if either $\tilde{f}_i = \tilde{c}_i$ or

$$\tilde{f}_i = \begin{cases} \tilde{a}_i \\ \tilde{b}_i \\ \tilde{d}_i \\ \tilde{n}_i \end{cases} \quad \text{and for all } \tilde{D}_j \in \begin{cases} \tilde{D}_R^{(i)} \\ \tilde{D}_L^{(i)} \\ \tilde{D}_R^{(i)} \\ \tilde{D}_R^{(i)} \end{cases}, \begin{cases} \{\tilde{b}_i, \tilde{n}_i\} \\ \{\tilde{b}_i, \tilde{a}_i\} \\ \{\tilde{c}_i, \tilde{d}_i\} \\ \{\tilde{d}_i, \tilde{n}_i\} \end{cases} \quad \not\subset \tilde{D}_j,$$

where we used Notation 4.19.

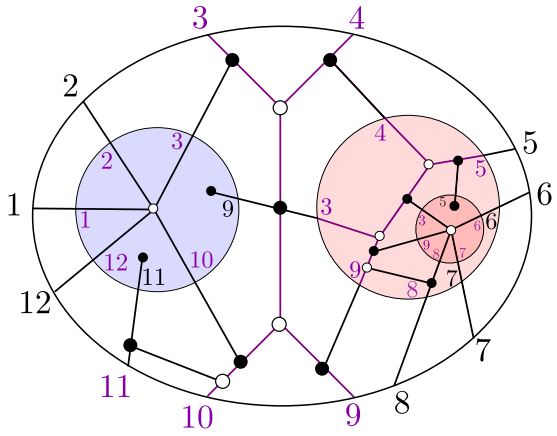

FIGURE 15.

Example 4.22. Consider the BCFW cell $S_{\mathfrak{r}}$ of Figure 6 and its generalized chords as in Example 4.20. The cell $S_{\mathfrak{r}}$ is $\tilde{f}_i$-condensable for all $\tilde{f}_i$ except for $\tilde{f}_i \in \{\tilde{d}_2, \tilde{n}_2, \tilde{b}_4\}$. For example, the cell is not $\tilde{d}_2$-condensable because $\{\tilde{c}_2, \tilde{d}_2\} = \{8, 9\} \subset \tilde{D}_1$, and $\tilde{D}_1$ is in $\tilde{D}_R^{(2)}$.

Definition 4.23. Let $S_{\mathfrak{r}} \subseteq \mathrm{Gr}_{k,n}^{\geq 0}$ be a BCFW cell, and $\tilde{D} = \{\tilde{D}_i\}_{i=1}^k$ the corresponding generalized chords. We define the *$\tilde{f}_i$-condensation* $\partial_{\tilde{f}_i} S_{\mathfrak{r}}$ of $S_{\mathfrak{r}}$ to be the cell built using the recipe $\mathfrak{r}$, but at the i-th BCFW product, we delete the edge e_1 if $\tilde{f}_i = \tilde{a}_i$; e_2 if $\tilde{f}_i = \tilde{b}_i$; e_3 if $\tilde{f}_i = \tilde{c}_i$; e_4 if $\tilde{f}_i = \tilde{d}_i$; and e_5 if $\tilde{f}_i = \tilde{n}_i$ as in Figure 16.

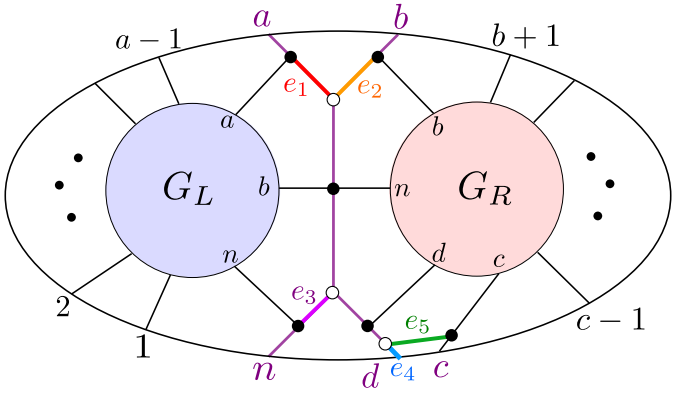

FIGURE 16.

Definition 4.24. Let $S_{\tilde{D}}$ be a general BCFW cell, with generalized chords $\tilde{D} = \{(\tilde{a}_j, \ldots, \tilde{n}_j)\}_{j=1}^k$. The $\tilde{f}_i$-condensation $\partial_{\tilde{f}_i} S_{\tilde{D}}$ of $S_{\tilde{D}}$ is *rigid* if for all $\ell > i$, $\{\tilde{b}_\ell, \tilde{c}_\ell, \tilde{d}_\ell, \tilde{n}_\ell\}$ is coindependent (as in Definition 4.2) for $\partial_{\tilde{f}_i} S_{\tilde{D}_R^{(\ell)}}$, where $\tilde{D}_R^{(\ell)}$ is as in Notation 4.19.

Using the techniques of this paper, and extending the ones used for the standard BCFW tiles, the following statement can be shown.

Claim 4.25 (Facets of general BCFW tiles)**.** Let $S = S_{\tilde{D}}$ be a BCFW cell with recipe $\mathfrak{r}$. If $S_{\tilde{D}}$ is $\tilde{f}_i$-condensable and $S' = \partial_{\tilde{f}_i} S_{\tilde{D}}$ is rigid, then $Z_{S'}$ is a facet of Z_S.

Moreover, let $\bar{\zeta}_i$ be the coordinate cluster variable of Z_S defined as

$$\bar{\zeta}_i = \begin{cases} \bar{\alpha}_i^{\mathfrak{r}}, \text{ if } \tilde{f}_i = \tilde{a}_i \\ \bar{\beta}_i^{\mathfrak{r}}, \text{ if } \tilde{f}_i = \tilde{b}_i \\ \bar{\gamma}_i^{\mathfrak{r}}, \text{ if } \tilde{f}_i = \tilde{c}_i \\ \bar{\delta}_i^{\mathfrak{r}}, \text{ if } \tilde{f}_i = \tilde{d}_i \\ \bar{\varepsilon}_i^{\mathfrak{r}}, \text{ if } \tilde{f}_i = \tilde{n}_i \end{cases} \quad \text{(see Definition 3.6)}, \tag{7}$$

then the facet $Z_{S'}$ is cut out by the functionary $\bar{\zeta}_i(Y)$. Finally, all facets of Z_S arise this way.

Remark 4.26. It can be shown that in case $\partial_{\tilde{\zeta}_i} S_{\tilde{D}}$ is not rigid, then for the minimal $l > i$ such that the condition in Definition 4.24 is not met, $\bar{\alpha}_l$ equals the BCFW coordinate $\bar{\zeta}_i$ of the i-th generalized chord which corresponds to $\tilde{f}_i$ according to Equation (7).

Example 4.27. Consider the example in Figure 6. All the condensations of the condensable cases in Example 4.22 are rigid. Therefore $S_{\mathfrak{r}}$ has 17 facets and they are cut out by all the functionaries in Example 3.9, except for $\bar{\delta}_2(Y), \bar{\varepsilon}_2(Y), \bar{\beta}_4(Y)$, corresponding to the non-condensable cases in Example 4.22.

We omit the proof of Claim 4.25 as it is similar to the proof of Theorem 4.1 in the standard BCFW case, but the technical details are much lengthier.

Remark 4.28. In the case of standard BCFW cells, the $\tilde{f}_i$-condensation is non-rigid only in the case of $\tilde{f}_i = \tilde{b}_i$ when D_i is a sticky same-end child of a chord D_p. In this case, $\bar{\beta}_i = \bar{\alpha}_p$ and $\bar{\beta}_i = \bar{\alpha}_p = 0$ does not cut out a facet. The non-condensable cases correspond precisely to the remaining mutable variables $\mathrm{Mut}(D)$ (cf. Definition 3.13).

5. The spurion tile and tiling

The amplituhedron $\mathcal{A}_{n,k,4}(Z)$ has a broad class of tiles, the *BCFW tiles* (cf. Definition 2.17). Moreover, we can use BCFW tiles to tile $\mathcal{A}_{n,k,4}(Z)$ into a broad class of tilings, the *BCFW tilings*, see [ELP$^+$23, Section 12]. We note that there are tilings made of BCFW tiles which are *not* BCFW tilings (e.g. cf. [ELP$^+$23, Theorem 12.6]). However, there are also tiles which are *not* BCFW tiles, and it turns out that they can also be used to tile $\mathcal{A}_{n,k,4}(Z)$. In this section we report the first example in the literature of a tiling containing a non-BCFW tile.

5.1. **Spurion tiles.** The simplest case of a tiling with non BCFW tiles is for $n = 9$ and $k = 2$, i.e. for $\mathcal{A}_{9,2,4}(Z)$. Consider the positroid cell $S_{sp} \subset \mathrm{Gr}^{\geq 0}_{2,9}$ with plabic graph in Figure 17.

A matrix C_{sp} representing a point in S_{sp} has triples of proportional columns whose labels are: $\{1,2,3\}, \{4,5,6\}, \{7,8,9\}$. We denote such configuration of column vectors as (123)(456)(789), see Appendix A. Therefore any such matrix representative has rows of support at least 6. We showed in [ELP$^+$23, Section 6] that points in a BCFW cells can be represented by matrices with at least one row of support 5. Therefore, S_{sp} is *not* a BCFW cell and we call it a *spurion* cell. By writing a parametrization with functionaries, and applying techniques from [ELP$^+$23], it is possible to show

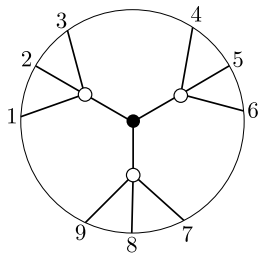

FIGURE 17. Plabic graph of the spurion cell $S_{sp} \subset \mathrm{Gr}_{2,9}^{\geq 0}$.

that the amplituhedron map is injective on S_{sp}, hence $Z_{sp} := \overline{\tilde{Z}(S_{sp})}$ is a tile for $\mathcal{A}_{9,2,4}(Z)$, which we call a *spurion* tile. This is an example of a non BCFW tile. Applying cyclic shifts to S_{sp} (Z_{sp}), we can obtain two other spurion cells (tiles) for $\mathcal{A}_{9,2,4}(Z)$.

5.2. **A tiling containing the spurion.** We are able to find a tiling $\mathcal{T}_{sp}$ of $\mathcal{A}_{9,2,4}(Z)$ containing a spurion tile. We report the collection of tiles in $\mathcal{T}_{sp}$ in Appendix A. Moreover, $\mathcal{T}_{sp}$ is a *good*[13] tiling of $\mathcal{A}_{9,2,4}(Z)$ and it is 'close' to a good BCFW tiling $\mathcal{T}_{BCFW}$. We report the collection of 5 tiles to substitute in order to go from $\mathcal{T}_{sp}$ to $\mathcal{T}_{BCFW}$ in Appendix A. We present a sketch of a proof in Section 5.3.1.

5.3. **Spurion tiles and cluster algebras.** The spurion tile exhibits the same relationship to the cluster structure on $\mathrm{Gr}_{4,n}$ as BCFW tiles. Firstly, Z_{sp} satisfies *cluster adjacency* in [ELP$^+$23, Conjecture 7.17(i)]. Indeed, Z_{sp} has 9 facets lying on the vanishing locus of the following collection $\mathcal{F}_{sp}$ of functionaries: $a_1(Y) = \langle\langle 123|65|789\rangle\rangle$, $a_2(Y) = \langle\langle 123|64|789\rangle\rangle$, $a_3(Y) = \langle\langle 123|54|789\rangle\rangle$, together with their cyclic shifts $(\mathrm{cyc}^*)^3$ and $(\mathrm{cyc}^*)^6$. The functionaries (up to sign) in $\mathcal{F}_{sp}$ correspond to a collection $\mathrm{Froz}(Z_{sp})$ of compatible cluster variables of $\mathrm{Gr}_{4,n}$ (see Notation 3.7). A seed $\tilde{\Sigma}_{sp}$ for $\mathrm{Gr}_{4,n}$ containing $\mathrm{Froz}(Z_{sp})$ was found in [GP23, Figure 1], see Figure 18.

Moreover, the open spurion tile $Z_{sp}^{\circ} \subset \mathrm{Gr}_{2,6}$ is fully determined by the functionaries in $\mathcal{F}_{sp}$ having a definite sign (see Figure 18). Therefore, the coordinate cluster variables $\mathbf{x}_{sp}$ are exactly the ones in $\mathrm{Froz}(Z_{sp})$ (containing the functionaries that cut out the facets of Z_{sp}). Let $\widetilde{\mathbf{x}}_{sp}$ denote the extended cluster of $\tilde{\Sigma}_{sp}$. We observe that all functionaries $x(Y)$ with x cluster variables in $\widetilde{\mathbf{x}}_{sp}$ have a definite sign on Z_{sp}. Furthermore, the seed obtained from $\tilde{\Sigma}_{sp}$ by freezing $\mathrm{Froz}(Z_{sp})$ is a *signed seed* [ELP$^+$23, Definition 9.22], hence Z_{sp} also satisfies the *positivity test* in [ELP$^+$23, Conjecture 7.17(ii)].

Remark 5.1 (Relation to Physics)**.** Spurion cells first appeared in [AHBC$^+$16a, Table 1]. They are informally called 'spurion' by physicists because they correspond to Yangian invariants (see, e.g. [ELP$^+$23, Remark 4.6]) which have only spurious poles, i.e. poles which cancel in the sum when computing the scattering amplitude. Geometrically, this is reflected in the fact the spurion tile, contrary to general BCFW tiles, does not have any facet which lie on the boundary of the amplituhedron.

It had been an open problem to determine whether tree-level scattering amplitudes in $\mathcal{N} = 4$ SYM could be expressed in terms of the spurion. By showing the amplituhedron $\mathcal{A}_{n,k,4}(Z)$ has

[13]meaning that internal facets of adjacent tiles match pairwise.

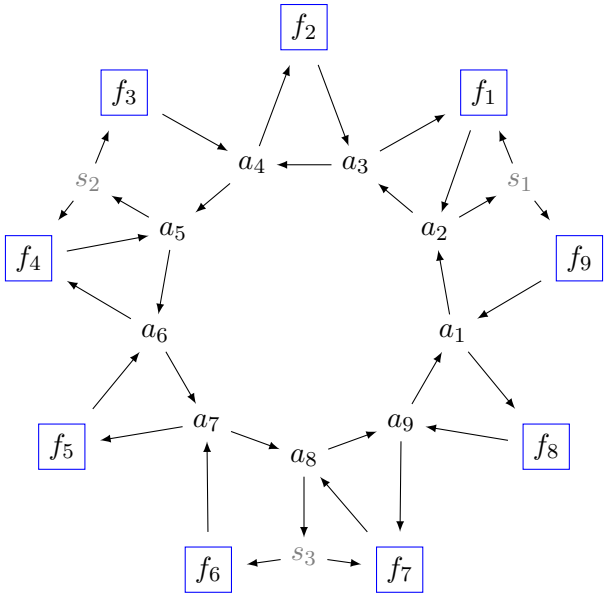

FIGURE 18. The seed $\tilde{\Sigma}_{sp}$, where: $a_1 = \langle 123|65|789\rangle$, $a_2 = \langle 123|64|789\rangle$, $a_3 = \langle 123|54|789\rangle$, $a_4 = \langle 789|23|456\rangle$, $a_5 = \langle 789|13|456\rangle$, $a_6 = \langle 789|12|456\rangle$, $a_7 = \langle 456|89|123\rangle$, $a_8 = \langle 456|79|123\rangle$, $a_7 = \langle 456|78|123\rangle$, $s_1 = \langle 1456\rangle$, $s_2 = \langle 1237\rangle$, $s_1 = \langle 4789\rangle$. The functionaries $a_2(Y), a_5(Y), a_8(Y)$ are positive on Z°_{sp} and all the others are negative.

tilings comprising the spurion tile, we solve this problem. The spurion tiling corresponds to a new expression of scattering amplitudes, which can not be obtained from physics via BCFW recursions.

5.3.1. *Sketch of a proof for the tiling with spurion.* We now sketch a proof that the spurion tiling of Appendix A is indeed a tiling.

- Let $S_\nu \subset \mathrm{Gr}^{\geq 0}_{2,6}$ be the 9 dimensional positroid cell labelled by the affine permutation $\nu = \{2,6,4,5,8,7,9,12,10\}$. S_ν has exactly 10 facets $S_1,\ldots,S_{10} \subset \overline{S}_\nu$ that map injectively to $\mathcal{A}_{9,2,4}(Z)$, giving the tiles $Z_{S_1},\ldots,Z_{S_{10}}$. Z_{S_1} is a spurion tile, and the remaining nine are BCFW tiles, five of which, $Z_{S_6},\ldots,Z_{S_{10}}$, are part of the BCFW tiling $\mathcal{T}_{BCFW}$. We now perform a *flip* on $\mathcal{T}_{BCFW}$ by replacing the tiles $Z_{S_6},\ldots,Z_{S_{10}}$ with $Z_{S_1},\ldots,Z_{S_5}$. Let $\mathcal{T}_{sp}$ be the resulting collection of tiles. We claim that $\mathcal{T}_{sp}$ is a tiling of $\mathcal{A}_{9,2,4}(Z)$ (which contains the spurion tile Z_{S_1}).

  In order to show the claim, it is enough to prove that $\{Z^{\circ}_{S_i}\}_{i=1}^{5}$ are pairwise disjoint and that

$$\bigcup_{i=1}^{5} Z_{S_i} = \bigcup_{i=6}^{10} Z_{S_i}. \tag{8}$$

  Let $\mathcal{F}'$ ($\mathcal{F}''$) denote the left (right) hand side of Equation (8).
- The tiles $Z_{S_6},\ldots,Z_{S_{10}}$ have the following facets: 15 'external' facets $Z_{B_1},\ldots,Z_{B_{15}}$, which cover the boundary of $\mathcal{F}''$; 10 'internal' facets, each of which belongs to a pair of tiles among $Z_{S_6},\ldots,Z_{S_{10}}$ which lie on opposite sides of it. Similarly, the tiles $Z_{S_1},\ldots,Z_{S_5}$ have the same 15 external facets $Z_{B_1},\ldots,Z_{B_{15}}$ and 10 internal facets $Z_{B'_1},\ldots,Z_{B'_{10}}$, each of which belongs to a pair of tiles among $Z_{S_1},\ldots,Z_{S_5}$.

- One can show that the functionaries vanishing on the internal facets serve as separating functionaries for all pairs of tiles in $\{Z_{S_i}\}_{i=1}^5$. In particular, if $Z_{B_i'}$ is a facet of both Z_{S_j} and Z_{S_r}, one can show the facet functionary of $Z_{B_i'}$ has definite opposite sign on $Z_{S_j}^\circ$ and $Z_{S_r}^\circ$ by using the Cauchy-Binet expansion for twistors (see, for example, [ELP$^+$23, Lemma 2.16]) and Plücker relations. Moreover, using similar techniques, one can show that each external facet Z_{B_i} belongs to a pair of tiles $Z_{S_{j'}} \subset \mathcal{F}'$ and $Z_{S_{j''}} \subset \mathcal{F}''$ and the corresponding facet functionary has definite same sign on $Z_{S_{j'}}^\circ$ and $Z_{S_{j''}}^\circ$.
- The previous arguments and a topological argument shows that the collection $\{Z_{S_i}\}_{i=1}^5$ tiles $\mathcal{F}'$, whose boundary is $\partial\mathcal{F}''$. Moreover, locally both $\mathcal{F}'$ and $\mathcal{F}''$ lie on the same side of such boundary. Since $\mathcal{F}', \mathcal{F}''$ are of the same dimension of the amplituhedron, by standard algebraic topology arguments (e.g. those of [ELT21, Section 8]), one can conclude that $\mathcal{F}' = \mathcal{F}''$. The claim follows. □

6. Standard BCFW tiles as positive parts of cluster varieties

In this section, we provide a birational map from $\mathrm{Gr}_{k,k+4}$ to a cluster variety $\mathcal{V}_D$ which maps an open standard BCFW tile Z_D° bijectively to the positive part of $\mathcal{V}_D$. The tile seed $\check{\Sigma}_D$ defining $\mathcal{V}_D$ is quasi-homomorphic to the seed Σ_D of [ELP$^+$23, Definition 9.8]. Throughout this section, we fix a chord diagram $D \in \mathcal{CD}_{n,k}$. In a mild abuse of notation, we use the terminology "domino variable" also for the functionary $x(Y)$ corresponding to a domino cluster variable $x \in \mathbf{x}(D)$.

First, recall we have two sets of functions which determine a point of the tile: the $5k$ coordinate functionaries and the $5k - t$ domino variables, where t is the number of chords of D which are sticky same-end children. It will be useful to express the coordinate functionaries of Z_D° in terms of the domino variables $\mathbf{x}(D)$. By definition, the coordinate functionaries are (signed) Laurent monomials in the domino variables. In the next proposition, we give explicit formulas for these Laurent monomials, up to sign. The signs may be computed using [ELP$^+$23, Proposition 8.10] and the fact that all coordinate functionaries are positive on the tile (cf. Theorem 3.10).

For a chord D_i in a chord diagram D, we set $E_i := \prod_\ell \bar{\varepsilon}_\ell$ where the product is over all ancestors of D_i which contribute to the expression $|c_i\ d_i \nearrow_i n\rangle$ (cf. [ELP$^+$23, Notation 8.3]). We define E_i' identically, but with the product over ancestors contributing to $|b_i\ c_i \nearrow_i n\rangle$.

Proposition 6.1. *Let $D \in \mathcal{CD}_{n,k}$ be a chord diagram. Then we have the following expressions for the coordinate functionaries of Z_D in terms of the domino variables:*

$$\alpha_i(Y) = \pm\frac{\bar{\alpha}_i}{E_i}, \qquad \beta_i(Y) = \pm\frac{(\bar{\beta}_i)(\bar{\alpha}_p)}{E_i}, \qquad \delta_i(Y) = \pm\frac{\bar{\delta}_i(\bar{\alpha}_p)}{E_i'}, \qquad \varepsilon_i(Y) = \pm\bar{\varepsilon}_i,$$

$$\gamma_i = \pm\frac{\bar{\gamma}_i(\bar{\alpha}_p)}{E_i(\bar{\delta}_p)(\bar{\beta}_j)(\bar{\varepsilon}_p)(\bar{\varepsilon}_g)}$$

where $(\bar{\alpha}_p)$ appears if D_i has a sticky parent D_p; $(\bar{\beta}_i)$ appears unless *D_i has a sticky and same-end parent; $(\bar{\delta}_p)$ appears if D_i has a same-end parent D_p; $(\bar{\beta}_j)$ appears if D_j is right head-to-tail sibling of D_i; $(\bar{\varepsilon}_p)$ appears if $(\bar{\beta}_j)$ appears and D_i has a sticky parent D_p which is not same-end to D_j; and $(\bar{\varepsilon}_g)$ appears if D_i has a same-end parent D_p and D_p has a sticky but not same-end parent D_g.*

Proposition 6.1 can be proved using the explicit formulas for domino variables [ELP$^+$23, Theorem 8.4] and [ELP$^+$23, Lemma 8.7] on factorization under promotion.

Example 6.2. For the chord diagram D in Figure 3, the formulas for coordinate functionaries in terms of domino variables are:

i	α_i	β_i	γ_i	δ_i	ε_i
1	$\frac{\bar\alpha_1}{\bar\varepsilon_3}$	$-\frac{\bar\beta_1}{\bar\varepsilon_3}$	$\frac{\bar\gamma_1}{\bar\beta_2\bar\varepsilon_3}$	$-\frac{\bar\delta_1}{\bar\varepsilon_3}$	$\bar\varepsilon_1$
2	$-\bar\alpha_2$	$\bar\beta_2$	$\frac{\bar\gamma_2}{\bar\delta_3\bar\beta_6}$	$\frac{\bar\delta_2}{\bar\varepsilon_3}$	$\bar\varepsilon_2$
3	$-\bar\alpha_3$	$\bar\beta_3$	$-\frac{\bar\gamma_3}{\bar\beta_6}$	$\bar\delta_3$	$\bar\varepsilon_3$
4	$\frac{\bar\alpha_4}{\bar\varepsilon_6}$	$-\frac{\bar\alpha_5}{\bar\varepsilon_6}$	$\frac{\bar\gamma_4\bar\alpha_5}{\bar\delta_5\bar\varepsilon_6^2}$	$-\frac{\bar\delta_4\bar\alpha_5}{\bar\varepsilon_5\bar\varepsilon_6}$	$\bar\varepsilon_4$
5	$-\frac{\bar\alpha_5}{\bar\varepsilon_6}$	$\frac{\bar\beta_5\bar\alpha_6}{\bar\varepsilon_6}$	$\frac{\bar\gamma_5\bar\alpha_6}{\bar\varepsilon_6}$	$-\frac{\bar\delta_5\bar\alpha_6}{\bar\varepsilon_6}$	$\bar\varepsilon_5$
6	$\bar\alpha_6$	$-\bar\beta_6$	$\bar\gamma_6$	$-\bar\delta_6$	$\bar\varepsilon_6$

Note that both the set of domino variables and the set of coordinate functionaries give redundant descriptions of the tile, which is $4k$ dimensional. We will use Lemma 6.3 to rescale the domino variables $\mathbf{x}(D)$ by (signed) Laurent monomials in $\mathrm{Froz}(D)$ to obtain $4k$ "tile variables." The tile variables form a coordinate system for Z_D°, are positive on Z_D°, and will comprise the cluster variables of $\check\Sigma_D$.

We perform this scaling in two steps. First, for a domino variable $\bar\zeta_i(Y)$, let s be the sign of $\bar\zeta_i(Y)$ on the open tile Z_D° (cf. [ELP$^+$23, Proposition 8.10]) and define the *signed domino variable* as $\hat\zeta_i(Y) := s\cdot\bar\zeta_i(Y)$. Note that each coordinate functionary is a Laurent monomial in the signed domino variables, given by the formulas in Proposition 6.1 by replacing each domino variable with a signed domino variable and deleting the signs. We denote by $\hat{\mathbf{x}}(D)$ the set of signed domino variables.

The second step of the scaling is more involved. The next proposition identifies the correct scaling factor $m(\hat\zeta_i)$ for each signed domino variable $\hat\zeta_i$, which will be a Laurent monomial in the $\hat\gamma_i$. The proof of this proposition gives an algorithm to determine the scaling factor.

We use the notation $\mathbb{M}[X]$ to denote the group of Laurent monomials in the variables X.

Lemma 6.3. *Let $\Gamma := \{\hat\gamma_i : D_i$ does not have a sticky same-end parent$\}$. There exists a unique group homomorphism $m : \mathbb{M}[\hat{\mathbf{x}}(D)] \to \mathbb{M}[\Gamma]$ such that*

(1) for $\hat\gamma_i \in \Gamma$, $m(\hat\gamma_i)$ is $\hat\gamma_i^{-1}$.
(2) for each $i \in [k]$, the image $m(\zeta_i)$ of the coordinate functionary $\zeta_i(Y)$ is equal for all $\zeta \in \{\alpha,\beta,\gamma,\delta,\epsilon\}$.

Moreover, the degree of $m(\hat\zeta_i)$ in twistor coordinates is equal to the degree of $\hat\zeta_i^{-1}$ in twistor coordinates for all $\hat\zeta_i \in \check{\mathbf{x}}(D)$.

Proof. A group homomorphism is uniquely determined by the images of $\hat{\mathbf{x}}(D)$. We will determine m on the signed domino variables $\hat\zeta_i(Y)$ for $i = k, k-1, \ldots, 1$, in that order. For the rest of this proof, "degree" means "degree in twistor coordinates."

We begin with the signed domino variables for the chord D_k. Note that $\hat{\gamma}_k \in \Gamma$ since D_k is a top chord. So (1) is satisfied if and only if $m(\hat{\gamma}_k) = \hat{\gamma}_k^{-1}$. Since D_k is a top chord, Proposition 6.1 implies that $\hat{\zeta}_k$ is equal to the coordinate functionary ζ_k. Thus (2) is satisfied if and only if $m(\hat{\zeta}_k) = \hat{\gamma}_k^{-1}$ for $\zeta \in \{\alpha, \beta, \gamma, \delta, \epsilon\}$. We see that when (1) and (2) hold, the degree of $\hat{\zeta}_k^{-1}$ is equal to the degree of $\hat{\gamma}_k^{-1}$.

Now, assume for all $\ell > i$ and all signed domino variables $\hat{\zeta}_\ell$ that there is a unique choice of image $m(\hat{\zeta}_\ell)$ so that (1) and (2) hold for ℓ, and the statement about degrees holds. We will show that there is also a unique choice of each image $m(\hat{\zeta}_i)$ so that (1) and (2) also hold for i, and that for this choice, the statement about degrees holds.

Case 1: If $\hat{\gamma}_i \notin \Gamma$ then (1) is vacuously true. Since D_i is a sticky same-end child of its parent D_p, we see from Proposition 6.1 that the coordinate functionary β_i is a Laurent monomial in signed domino variables $\hat{\zeta}_\ell$ where $\ell > i$. Thus the image $m(\beta_i)$ is determined by the values of $m(\hat{\zeta}_\ell)$. For (2) to hold, we must have $m(\beta_i) = m(\zeta_i)$ for all other coordinate functionaries ζ_i. Again by Proposition 6.1, $\zeta_i = \hat{\zeta}_i \cdot M$ where M is a Laurent monomial in signed domino variables for $\ell > i$. So (2) holds if and only if $m(\hat{\zeta}_i) = m(\beta_i)/m(M)$.

For the statement about degrees, notice first that the coordinate functionaries ζ_i are degree 1, because they are promotions of twistor coordinates and promotion preserves degree. The assumption on the degrees of $m(\hat{\zeta}_\ell)$ implies that the degree of $m(\beta_i)$ is -1. Since $\zeta_i = \hat{\zeta}_i \cdot M$, the degree of $\hat{\zeta}_i$ is $1 - \deg(M)$. On the other hand, $m(\hat{\zeta}_i) = m(\beta_i)/m(M)$ implies that the degree of $m(\hat{\zeta})$ is $-1 - \deg m(M)$, which is equal to $-1 + \deg(M)$ by the assumption on the degrees of $m(\hat{\zeta}_\ell)$. So we have the desired equality of degrees.

Case 2: If $\hat{\gamma}_i \in \Gamma$, then (1) holds if and only if $m(\hat{\gamma}_i) = \hat{\gamma}_i^{-1}$. The statement about degrees clearly holds for $\hat{\gamma}_i$. The choice of $m(\hat{\gamma}_i)$ completely determines the image $m(\gamma_i)$ of the coordinate functionary γ_i, using Proposition 6.1. Similar reasoning as the above case shows that there is a unique choice of $m(\hat{\zeta}_i)$ so that (2) holds, and that the statement about degrees holds for this choice. □

Definition 6.4 (Tile variables and seeds)**.** Let m be as in Lemma 6.3. For each signed domino variable $\hat{\zeta}_i(Y) \in \hat{\mathbf{x}}(D) \setminus \Gamma$, we define the *tile variable* as $\check{\zeta}_i(Y) := m(\hat{\zeta}_i(Y)) \cdot \hat{\zeta}_i(Y)$. We denote by $\check{\mathbf{x}}(D)$ the set of tile variables. We define the *tile seed* $\check{\Sigma}_D = (\check{\mathbf{x}}(D), \check{Q}_D)$ as the seed obtained from Σ_D by deleting $\{\bar{\gamma}_i : \bar{\gamma}_i \notin \Gamma\}$, and replacing each domino variable $\bar{\zeta}_i$ by the corresponding tile variable $\check{\zeta}_i(Y)$. Finally, we let $\mathcal{A}(\check{\Sigma}_D)$ be the associated cluster algebra, which we call *tile cluster algebra*.

Each tile variable is positive on Z_D°, there are exactly $4k = \dim Z_D^\circ$ tile variables, and each tile variable is degree 0 in the twistor coordinates. It will sometimes be convenient to extend the definition of tile variables to $\hat{\zeta}_i \in \Gamma$; in this case $\check{\zeta}_i(Y) := 1$.

Example 6.5 (Tile cluster variables)**.** For the chord diagram D in Figure 3, the domino variables

$$\bar{\alpha}_2,\ \bar{\alpha}_3,\ \bar{\alpha}_5 = \bar{\beta}_4,\ \bar{\beta}_1,\ \bar{\beta}_6,\ \bar{\gamma}_2,\ \bar{\delta}_1,\ \bar{\delta}_5,\ \bar{\delta}_6$$

are negative on the tile Z_D°, and all others are positive (cf. Example 3.20). So the signed domino variable $\hat{\zeta}_i$ coincides with the domino variable $\bar{\zeta}_i$ unless $\bar{\zeta}_i$ is one of the variables listed above. To

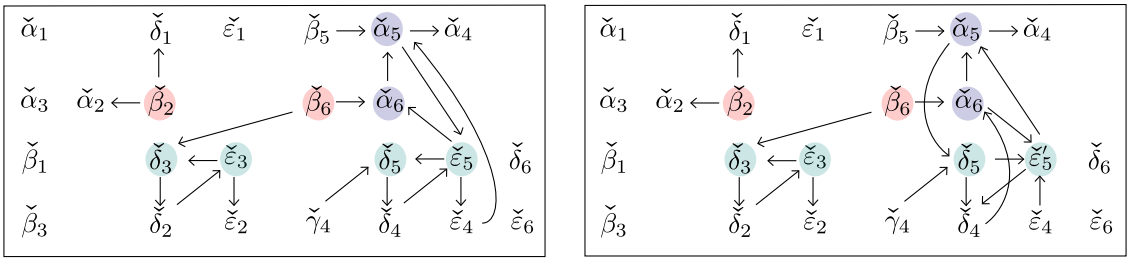

FIGURE 19. (Left): the tile seed $\check{\Sigma}_D$ for D in Figure 3. See Examples 3.12 and 6.5 for the formulas for the tile variables $\check{\zeta}_i$. (Right): the mutation of $\check{\Sigma}_D$ at $\check{\varepsilon}_5$.

obtain the tile cluster variable $\check{\zeta}_i$ for D, multiply $\hat{\zeta}_i$ by the monomial $m(\hat{\zeta}_i)$ listed in the table below.

i	$m(\hat{\alpha}_i)$	$m(\hat{\beta}_i)$	$m(\hat{\gamma}_i)$	$m(\hat{\delta}_i)$	$m(\hat{\varepsilon}_i)$
1	$\hat{\gamma}_2\hat{\gamma}_6(\hat{\gamma}_1\hat{\gamma}_3)^{-1}$	$\hat{\gamma}_2\hat{\gamma}_6(\hat{\gamma}_1\hat{\gamma}_3)^{-1}$	$\hat{\gamma}_1^{-1}$	$\hat{\gamma}_2\hat{\gamma}_6(\hat{\gamma}_1\hat{\gamma}_3)^{-1}$	$\hat{\gamma}_2\hat{\gamma}_1^{-1}$
2	$\hat{\gamma}_3(\hat{\gamma}_2\hat{\gamma}_6)^{-1}$	$\hat{\gamma}_3(\hat{\gamma}_2\hat{\gamma}_6)^{-1}$	$\hat{\gamma}_2^{-1}$	$\hat{\gamma}_2^{-1}$	$\hat{\gamma}_3(\hat{\gamma}_2\hat{\gamma}_6)^{-1}$
3	$\hat{\gamma}_6(\hat{\gamma}_3)^{-1}$	$\hat{\gamma}_6(\hat{\gamma}_3)^{-1}$	$\hat{\gamma}_3^{-1}$	$\hat{\gamma}_6(\hat{\gamma}_3)^{-1}$	$\hat{\gamma}_6(\hat{\gamma}_3)^{-1}$
4	$(\hat{\gamma}_5\hat{\gamma}_6)^{-1}$	$(\hat{\gamma}_5\hat{\gamma}_6)^{-1}$	$(\hat{\gamma}_5\hat{\gamma}_6)^{-1}$	$\hat{\gamma}_5^{-1}$	$\hat{\gamma}_5^{-1}$
5	$(\hat{\gamma}_5\hat{\gamma}_6)^{-1}$	$\hat{\gamma}_5^{-1}$	$\hat{\gamma}_5^{-1}$	$\hat{\gamma}_5^{-1}$	$\hat{\gamma}_5^{-1}$
6	$\hat{\gamma}_6^{-1}$	$\hat{\gamma}_6^{-1}$	$\hat{\gamma}_6^{-1}$	$\hat{\gamma}_6^{-1}$	$\hat{\gamma}_6^{-1}$

The tile seed $\check{\Sigma}_D$ is displayed on the left in Figure 19.

As the next result shows, the tile variables give coordinates on the open tile.

Proposition 6.6. *The map $f : Z_D^\circ \mapsto \mathbb{R}_+^{\check{\mathbf{x}}(D)}$ sending a point $Y \mapsto (\check{\zeta}_i(Y))$ to its list of tile variables is a bijection.*

Proof. We first show that each point in $\mathbb{R}_+^{\check{\mathbf{x}}(D)}$ has a preimage in Z_D°. Recall that Proposition 6.1 gives formulas for each coordinate functionary $\zeta_i(Y)$ as a Laurent monomial $N_{\zeta_i}(\hat{\zeta}_j(Y))$ in the signed domino variables. We define a Laurent monomial map

$$F : \mathbb{R}_+^{\check{\mathbf{x}}(D)} \to (\mathbb{R}_+)^{5k}$$

sending $(\check{\zeta}_i) \in \mathbb{R}_+^{\check{\mathbf{x}}(D)}$ to $(\zeta_i' := N_{\zeta_i}(\check{\zeta}_j))$, where the latter set ranges over all coordinate functionaries. That is, we evaluate the Laurent monomials N_{ζ_i} for coordinate functionaries in terms of signed domino variables on the tuple $(\check{\zeta}_i)$. (We set $\check{\zeta}_j := 1$ if $\hat{\zeta}_j(Y) \in \Gamma$.) For a point $p \in \mathbb{R}_+^{\check{\mathbf{x}}(D)}$, define $M_p := M_D(F(p))$ to be the BCFW matrix using $\{\zeta_i'\}$ as BCFW coordinates. We claim that $Y_p := \tilde{Z}(M_p) \in Z_D^\circ$ is a preimage of p under f. That is, the tile variables of Y_p are precisely p.

Recall that the rowspan of the BCFW matrix depends only on the projection of $F(p)$ to $(\mathrm{Gr}_{1,5}^{>0})^k$. We define a vector $q \in (\mathbb{R}_+)^{5k}$ whose entries are ζ_i' if D_i has a sticky same-end parent and are ζ_i'/γ_i' otherwise. By construction, q and $F(p)$ project to the same point. So the rowspan of M_p is equal to the rowspan of $M_D(q)$, and thus (the rowspan of) Y_p is also equal to (the rowspan of) $Y_q := \tilde{Z}(M_D(q))$. Theorem 3.10, and in particular the proof of [ELP+23, Proposition 11.15], implies that the coordinate functionaries of Y_q are exactly equal to the BCFW coordinates of $M_D(q)$; that is, the coordinate functionaries of Y_q are the entries of the vector q. Moreover, the twistor coordinates

of Y_p and Y_q differ by a global scalar. Because coordinate functionaries are degree 1 in twistors, the coordinate functionaries of Y_p and Y_q also differ by a global scalar. So $\zeta_i(Y_p) = c \cdot \zeta'_i/\gamma'_i$ if D_i does not have a sticky same-end parent and $\zeta_i(Y_p) = c \cdot \zeta'_i$ otherwise.

We need to show that $\check{\zeta}_i(Y_p)$, a function evaluated on Y_p, is equal to $\check{\zeta}_i$, which is either a coordinate of p or equal to 1. We will show this for $i = k, k-1, \ldots, 1$.

For $i = k$, since D_k is a top chord, for any $Y \in Z_D^\circ$

$$\zeta_k(Y) = \hat{\zeta}_k(Y) \quad \text{so} \quad \check{\zeta}_k(Y) = \zeta_k(Y)/\gamma_k(Y).$$

Setting $Y = Y_p$, we obtain $\check{\zeta}_k(Y_p) = \zeta'_k/\gamma'_k$. In this case, according to the definition of F, we have $\check{\zeta}_k = \zeta'_k$. In particular, $\gamma'_k = 1$. So we have $\check{\zeta}_k(Y_p) = \zeta'_k = \check{\zeta}_k$.

Assume $\check{\zeta}_\ell = \check{\zeta}_\ell(Y_p)$ for $\ell > i$.

Case 1: Suppose that D_i has a sticky same-end parent. For any $Y \in Z_D^\circ$, we have that $N_{\beta_i}(\check{\zeta}_j(Y)) = m(\beta_i(Y))\beta_i(Y)$ and the only tile variables appearing in the Laurent monomial on the left hand side are for chords D_ℓ with $\ell > i$. So, for $Y = Y_p$, we have $m(\beta_i(Y_P)) \cdot c\beta'_i = N_{\beta_i}(\check{\zeta}_j) = \beta'_i$, implying that $m(\beta_i(Y_P)) = c^{-1}$. For $\zeta_i \neq \beta_i$, we have

$$N_{\zeta_i}(\check{\zeta}_j(Y_P)) = m(\beta_i(Y_P))\zeta_i(Y_P) = \zeta'_i = N_{\zeta_i}(\check{\zeta}_j).$$

In the second equality, we use property (2) of the map m. Since $N_{\zeta_i}(\check{\zeta}_j(Y))$ is $\check{\zeta}_i(Y)$ times tile variables for $\ell > i$ and $\check{\zeta}_\ell = \check{\zeta}_\ell(Y_p)$ for $\ell > i$, the above string of equalities implies that $\check{\zeta}_i(Y_P)$ is equal to $\check{\zeta}_j$.

Case 2: Suppose D_i does not have a sticky same-end parent. Then $\check{\gamma}_i(Y) = 1 = \check{\gamma}_i$, since $\check{\gamma}_i(Y) \in \Gamma$. This means that $\gamma'_i = N_{\gamma_i}(\check{\zeta}_j(Y_p))$. On the other hand, $N_{\gamma_i}(\check{\zeta}_j(Y_p)) = m(\gamma_i(Y_p))\gamma_i(Y_p) = m(\gamma_i(Y_p))c$, so $c = \gamma'_i/m(\gamma_i(Y_p))$. For $\zeta_i \neq \gamma_i$, we have

$$N_{\zeta_i}(\check{\zeta}_j(Y_p)) = m(\gamma_i(Y_p))\zeta_i(Y_p) = c \cdot m(\gamma_i(Y_p))\zeta'_i/\gamma'_i = \zeta'_i = N_{\zeta_i}(\check{\zeta}_j).$$

Again, in the second equality, we use property (2) of the map m. By a similar argument as in the first case, this shows that $\check{\zeta}_i(Y_p) = \check{\zeta}_i$.

This shows that Y_p is a preimage of p in Z_D°. For uniqueness, note that the tile variables determine the coordinate functionaries up to a scalar for each i. So another preimage Y' would have coordinate functionaries $\zeta_i(Y')$ which can only differ from $\zeta_i(Y_p)$ by a scalar c_i. However, this implies that the twistor matrix $M_D(Y')$ has the same rowspan as the twistor matrix $M_D(Y_p)$, and thus $Y' = \tilde{Z}(M_D(Y'))$ is equal to $Y_p = \tilde{Z}(M_D(Y_p))$.

□

One may upgrade Proposition 6.6 to a statement about the cluster variety $\mathcal{V}_D$ corresponding to the tile seed $\check{\Sigma}_D$ as follows.

Theorem 6.7. *Let $f : \mathrm{Gr}_{k,k+4} \dashrightarrow \mathcal{V}_D$ be the map $Y \mapsto (\check{\zeta}_i(Y))$ sending a point to its list of tile variables. Then f is a birational map which maps Z_D° onto the positive part of $\mathcal{V}_D$.*

Proof. Let $T_D \subset \mathrm{Gr}_{k,k+4}$ be the subset where all tile variables are well-defined and nonvanishing. Note that T_D is open and nonempty, as it contains Z_D°. The map f is well-defined on T_D, and the tile coordinates are rational functions in the Plücker coordinates of Y, so f is rational. Note that $f(T_D)$ is contained in the cluster torus $T_{\check{\Sigma}_D} = (\mathbb{C}^*)^{\check{\mathbf{x}}(D)} \subset \mathcal{V}_D$.

In the proof of Proposition 6.6, we constructed an inverse to f on the positive part $\mathbb{R}_+^{\check{\mathbf{x}}(D)}$ of $\mathcal{V}_D$. This inverse extends to an open subset of the cluster torus $T_{\check{\Sigma}_D}$. Indeed, for $p \in T_{\check{\Sigma}_D}$, define M_p and Y_p as in the proof of Proposition 6.6. The matrix M_p is full-rank by e.g. [MS17], as it is the path matrix of a plabic graph with nonzero complex edge weights. However, Y_p may or may not be full rank. Let $T' \subset T_{\check{\Sigma}_D}$ be the subset of points p such that the coordinate functionaries of Y_p are well-defined and non-vanishing. The coordinate functionaries of Y_p are rational functions in the coordinates of p; if they are all well-defined and non-vanishing, then in particular Y_p has at least one nonvanishing twistor coordinate, and so is full rank. The tile variables can be expressed as Laurent monomials in the signed domino variables, and so also as Laurent monomials in coordinate functionaries. Thus, if the coordinate functionaries of Y_p are non-vanishing, so are the tile variables. This implies for $p \in T'$, $Y_p \in T_D$. Note that T' contains the positive part of $\mathcal{V}_D$, and so is open in $\mathcal{V}_D$.

We claim that $p \mapsto Y_p$ is the inverse of f on T'. The argument is very similar to the proof of Proposition 6.6. We outline the additional arguments needed. First, allowing the BCFW coordinates to vary over $(\mathrm{Gr}_{1,5})^k$ rather than $(\mathrm{Gr}_{1,5}^{>0})^k$, the BCFW matrices will parametrize a torus containing S_D [MS17]. Second, for any point $Y \in \mathrm{Gr}_{k,k+4}$ which has all non-vanishing coordinate functionaries, the proof of [ELP$^+$23, Proposition 11.15] shows that the unique pre-image of Y in this torus is given by the twistor matrix $M_D(Y)$. That is, the BCFW coordinates of this unique pre-image are exactly the coordinate functionaries of Y. With these facts in hand, the proof of Proposition 6.6 goes through identically for $p \in T'$. As the Plücker coordinates of Y_p are rational functions in the coordinates of p, $p \mapsto Y_p$ is rational.

Finally, Proposition 6.6 shows that f maps Z_D° onto the positive part of $\mathcal{V}_D$.

□

It would be interesting to upgrade Theorem 6.7 to a biregular map $T_D \to T_{\check{\Sigma}_D}$, or to an embedding $\mathcal{V}_D \hookrightarrow \mathrm{Gr}_{k,k+4}$.

For each cluster in the tile cluster algebra $\mathcal{A}(\check{\Sigma}_D)$, Theorem 6.7 gives a way to describe Z_D° as a semi-algebraic set, this time using dimension-many inequalities:

Corollary 6.8 (Positivity test)**.** *We have*

$$Z_D^\circ = \{Y \in \mathrm{Gr}_{k,k+4} : x(Y) > 0 \text{ for all } x \text{ in any fixed cluster of } \mathcal{A}(\check{\Sigma}_D)\}$$

In particular, $Y \in \mathrm{Gr}_{k,k+4}$ is in Z_D° if and only if all tile variables are positive on Y.

Proof. All cluster variables in $\mathcal{A}(\check{\Sigma}_D)$ are positive on Z_D° by construction, so it suffices to show the right hand side is contained in the left-hand side. If Y is in the right-hand side, then $f(Y)$ is in the positive part of $\mathcal{V}_D$. The inverse of f maps the positive part to Z_D°, so $Y \in Z_D^\circ$. □

7. Canonical forms of BCFW tiles from cluster algebra

In this section we use the cluster structure for BCFW tiles to compute the canonical form of such tiles purely in terms of cluster variables for $\mathrm{Gr}_{4,n}$.

7.1. **Background on Positive Geometry.**

Definition 7.1 ([AHBL17])**.** Let X be a d-dimensional complex irreducible algebraic variety which is defined over $\mathbb{R}$, and let $X^{\geq 0}$ be a closed[14] semialgebraic subset of $X(\mathbb{R})$, whose interior $X^{>0}$ is a d-dimensional oriented real manifold. Let $C_1 \dots C_r$ be the irreducible components of the Zariski-closure of the boundary $X^{\geq 0} \setminus X^{>0}$, and for $1 \leq i \leq r$ let $C_i^{\geq 0}$ denote the closure of the interior of $C_i \cap X^{\geq 0}$. We say that $(X, X^{\geq 0})$ is a *positive geometry* of dimension d if there exists a unique nonzero rational d-form $\Omega(X, X^{\geq 0})$ called the *canonical form*, satisfying the recursive axioms:

- If $d = 0$, then $X = X_{\geq 0} = \text{pt}$ is a point, and we define $\Omega = \pm 1$ depending on the orientation.
- If $d > 0$, then we require that $\Omega(X, X_{\geq 0})$ has poles only along the boundary components C_i, these poles are simple, and for each $1 \leq i \leq r$, we have that $(C_i, C_i^{\geq 0})$ is a positive geometry of dimension $d-1$, called a *facet* of $(X, X^{\geq 0})$, and

$$\text{Res}_{C_i} \Omega(X, X^{\geq 0}) = \Omega(C_i, C_i^{\geq 0}).$$

Example 7.2 ($d = 1$)**.** $(\mathbb{P}^1, [a, b])$, with the canonical form $\Omega = \frac{b-a}{(x-a)(b-x)} \mathrm{d}x$ is a positive geometry (closed interval). Its facets are: $(\{a\}, \{a\}), (\{b\}, \{b\})$ and $\text{Res}_a \Omega = 1, \text{Res}_b \Omega = -1$.

Example 7.3 ($d = 2$)**.** $(\mathbb{P}^2, \square_{1234})$, where $\square_{1234}$ is a quadrilateral with vertices $v_1 = (0, 0); v_2 = (2, 0); v_3 = (1, 2), v_4 = (0, 1)$, see Figure 20. The canonical form is:

$$\Omega(\mathbb{P}^2, \square_{1234}) = \frac{y - 4x - 4}{xy(y - x - 1)(2x + y - 4)} \mathrm{d}x \wedge \mathrm{d}y. \tag{9}$$

The facets are: $(\mathbb{P}^1, [v_1, v_2])$, $(\mathbb{P}^1, [v_2, v_3])$, $(\mathbb{P}^1, [v_3, v_4])$, $(\mathbb{P}^1, [v_4, v_1])$.

$$\text{Res}_{[v_1, v_2]} \Omega(\mathbb{P}^2, \square_{1234}) = \frac{2}{x(2 - x)} \mathrm{d}x = \Omega(\mathbb{P}^1, [v_1, v_2]).$$

$(\mathbb{P}^2, \text{half disk})$ with $\Omega = \frac{1}{y(x^2+y^2-1)} \mathrm{d}x \wedge \mathrm{d}y$ is a positive geometry. A closed disk is *not* a positive geometry. For more positive geometries in $d = 2$ see the work on *planar polypols* [KPR+21].

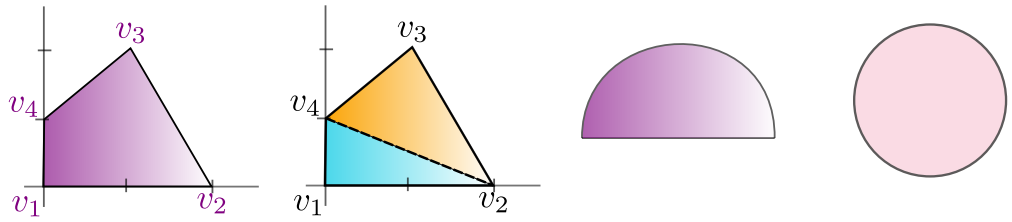

FIGURE 20. From left to right: the quadrilateral $\square_{1234}$; the tiling of $\square_{1234}$ into the triangles $\Delta_{124}, \Delta_{234}$; half disk; closed disk.

Definition 7.4. Let $(X, X^{\geq 0})$ be a positive geometry. A collection $\{(X_i, X_i^{\geq 0})\}_{i \in \mathcal{C}}$ of positive geometries is a *tiling* of $(X, X^{\geq 0})$ if:

- the interiors $X_i^{>0}$ are pairwise disjoint;
- the union $\cup_i X_i^{\geq 0}$ equals $X^{\geq 0}$;
- the orientation of each $X_i^{>0}$ agrees with $X^{>0}$.

[14]We always use the Euclidean topology, unless specified otherwise (e.g. in the case of Zariski topology).

Heuristic 7.5. [AHBL17] Let $(X, X^{\geq 0})$ be a positive geometry and the collection $\{(X_i, X_i^{\geq 0})\}_{i\in\mathcal{C}}$ be a tiling of $(X, X^{\geq 0})$. Then

$$\Omega(X, X^{\geq 0}) = \sum_{i\in\mathcal{C}} \Omega(X_i, X_i^{\geq 0}). \tag{10}$$

Example 7.6. $(\mathbb{P}^2, \square_{1234})$ can be tiled by the two triangles $(\mathbb{P}^2, \Delta_{124})$ and $(\mathbb{P}^2, \Delta_{234})$ with vertices (v_1, v_2, v_4) and (v_2, v_3, v_4) respectively, see Figure 20. Their canonical forms are:

$$\Omega(\Delta_{124}) = \frac{2}{xy(2-x-2y)}\mathrm{d}x\wedge\mathrm{d}y, \quad \Omega(\Delta_{234}) = \frac{9}{(1+x-y)(4-2x-y)(2-x-2y)}\mathrm{d}x\wedge\mathrm{d}y.$$

Then $\Omega(\square_{1234}) = \Omega(\Delta_{124}) + \Omega(\Delta_{234})$, cf. Equation (9). Moreover, the ('spurious') pole along the facet (24) cut out by $2-x-2y=0$ cancels in the sum. Indeed, (24) is not a facet of $\square_{1234}$.

Theorem 7.7. [AHBL17, KR20] *Let $\mathcal{P}$ be a projective pointed polyhedral cone (or projective polytope) in $\mathbb{P}^m$. Then $(\mathbb{P}^m, \mathcal{P})$ is a positive geometry. Moreover,*

$$\Omega(\mathbb{P}^m, \mathcal{P}) = \frac{N(x)}{D(x)} d^m x,$$

where $D(x)$ is the product of linear forms defining facets of $\mathcal{P}$, and $N(x)$ is the adjoint *of $\mathcal{P}$.*

The *adjoint* is a polynomial that cancels the 'unwanted' poles outside the polyope, i.e. it cuts out the hypersurface which passes through the *residual hyperplane arrangement* of $\mathcal{P}$.

Theorem 7.8. [Pos06, KLS13, Lam22] *$(Gr_{k,n}(\mathbb{C}), Gr_{k,n}^{\geq 0})$ is a positive geometry with canonical form:*

$$\Omega(\mathrm{Gr}_{k,n}(\mathbb{C}), \mathrm{Gr}_{k,n}^{\geq 0}) = \frac{d^{k(n-k)}C}{\langle 1,\dots,k\rangle\langle 2,\dots,k+1\rangle\dots\langle n,1,\dots,k-1\rangle},$$

where $\langle I\rangle$ denotes the Plücker coordinate of a point $C \in Gr_{k,n}^{\geq 0}$. Moreover, the faces $(\Pi_S(\mathbb{C}), \bar{S})$ are positive geometries, where $S \subset Gr_{k,n}^{\geq 0}$ is a positroid cell and $\Pi_S(\mathbb{C})$ is its Zariski closure in $Gr_{k,n}(\mathbb{C})$, called the positroid variety *of S.*

7.2. **The canonical form of the amplituhedron.** Both (cyclic) polytopes and the positive Grassmannian are positive geometries. These objects can also be seen as special cases of amplituhedra (in particular, the amplituhedra $\mathcal{A}_{n,1,m}(Z)$ and $\mathcal{A}_{n,n-m,m}(Z)$, respectively). Since the amplituhedron $\mathcal{A}_{n,k,m}(Z)$ is a subset of $\mathrm{Gr}_{k,k+m}$, it is natural to conjecture the following.

Conjecture 7.9. [AHBL17] *The amplituhedron $(\mathrm{Gr}_{k,k+m}(\mathbb{C}), \mathcal{A}_{n,k,m}(Z))$ is a positive geometry.*

In order to find the canonical form of the amplituhedron, one method is to tile $\mathcal{A}_{n,k,m}(Z)$ and sum over the canonical forms of the tiles (cf. Heuristic 7.5).

Definition 7.10 (Candidate canonical form of a tile)**.** Let Z_S be a tile of $\mathcal{A}_{n,k,m}(Z)$. As the amplituhedron map $\tilde{Z}$ is injective on the open tile Z_S°, we can define its inverse $\tilde{Z}^{-1} : Z_S^\circ \to S$. Then let us consider the pullback of the canonical form of the positroid cell under $\tilde{Z}^{-1}$:

$$\tilde{\Omega}(Z_S) = (\tilde{Z}^{-1})^*\Omega(\Pi_S(\mathbb{C}), \bar{S}). \tag{11}$$

We call $\tilde{\Omega}(Z_S)$ the[15] *candidate canonical form of the tile Z_S.*

[15]we will always consider it up to a global sign, which is not relevant for our paper and depends on the orientation.

By Theorem 7.8, $(\Pi_S(\mathbb{C}), \bar{S})$ is positive geometry and has a canonical form $\Omega(\Pi_S(\mathbb{C}), \bar{S})$. Moreover, by [AHT14, Section 6] and [GL20, Section 8.2], Equation (11) is well-defined.

Each positroid cell S has a positive parameterization [Pos06], i.e. there is a diffeomorphism $h : S \to \mathbb{R}_+^{mk}$ which sends a matrix representative C in S to a collection of positive coordinates $(\alpha_1, \ldots, \alpha_{mk})$ in $\mathbb{R}_+^{mk}$. In this case, if we denote $\phi = h \circ \tilde{Z}^{-1}$, then

$$\tilde{\Omega}(Z_S) = \phi^* \bigwedge_{i=1}^{mk} \mathrm{d}\log(\alpha_i). \tag{12}$$

Conjecture 7.11 (Tiles are positive geometries)**.** *Let Z_S be a tile of $\mathcal{A}_{n,k,m}(Z)$. Then $(\mathrm{Gr}_{k,k+m}(\mathbb{C}), Z_S)$ is a positive geometry and its canonical form $\Omega(\mathrm{Gr}_{k,k+m}(\mathbb{C}), Z_S)$ is the candidate canonical form $\tilde{\Omega}(Z_S)$ in Definition 7.10.*

Conjecture 7.12 (Canonical form from tilings)**.** *Let $\{Z_S\}_{S\in\mathcal{C}}$ be a tiling of $\mathcal{A}_{n,k,m}(Z)$. Then the canonical form of the amplituhedron $\mathcal{A}_{n,k,m}(Z)$ is obtained as*

$$\Omega(\mathrm{Gr}_{k,k+m}(\mathbb{C}), \mathcal{A}_{n,k,m}(Z)) = \sum_{S\in\mathcal{C}} \Omega(\mathrm{Gr}_{k,k+m}(\mathbb{C}), Z_S). \tag{13}$$

In particular, the right hand side of Equation (13) *is independent of the tiling.*

Remark 7.13. Clearly finding tilings of the amplituhedron and inverting the amplituhedron map on tiles are crucial step for computing the canonical form of the amplituhedron, and hence scattering amplitudes. In this paper and in [ELP$^+$23] we inverted the amplituhedron map [ELP$^+$23, Theorem 7.7] on *BCFW tiles* and proved the existence of a large family of tilings, the *BCFW tilings* [ELP$^+$23, Theorem 12.3]. It then follows from [MS09, AHCCK10, AHBC$^+$16b, AHT14] that tree-level scattering amplitudes in $\mathcal{N} = 4$ SYM expressed via BCFW recursions are computed by the sum of the candidate canonical forms of the tiles in a BCFW tiling of $\mathcal{A}_{n,k,4}(Z)$.

Proposition 7.14 (Canonical form of tiles from coordinate functionaries)**.** *Let $Z_{\mathfrak{r}}$ be a BCFW tile and $([\alpha_i(Y) : \beta_i(Y) : \gamma_i(Y) : \delta_i(Y) : \varepsilon_i(Y)])_{i=1}^k$ its associated coordinate functionaries as in* [ELP$^+$23, Definition 7.1]*. Then the candidate canonical form $\tilde{\Omega}(Z_{\mathfrak{r}})$ of $Z_{\mathfrak{r}}$ is given by:*

$$\tilde{\Omega}(Z_S) = \bigwedge_{i=1}^{k} dlog\frac{\beta_i(Y)}{\alpha_i(Y)} \wedge dlog\frac{\gamma_i(Y)}{\alpha_i(Y)} \wedge dlog\frac{\delta_i(Y)}{\alpha_i(Y)} \wedge dlog\frac{\epsilon_i(Y)}{\alpha_i(Y)}. \tag{14}$$

Analogously, for each $i \in [k]$, we could have chosen any other coordinate functionary $\zeta_i(Y)$ instead of $\alpha_i(Y)$ to divide the others by.

Proof. Given a BCFW tile $Z_{\mathfrak{r}}$, the inverse of the amplituhedron map $\tilde{Z}^{-1}$ sends a point Y in $Z_{\mathfrak{r}}^\circ$ to a point in $\mathrm{Gr}_{k,n}^{\geq 0}$ represented by the twistor matrix $M_{\mathfrak{r}}^{\mathrm{tw}}(Y)$ [ELP$^+$23, Definition 7.1]. Moreover, there is a positive parametrization of $S_{\mathfrak{r}}$ in terms of BCFW parameters $([\alpha_i : \beta_i : \gamma_i : \delta_i : \varepsilon_i])_{i=1}^k$ in $(\mathrm{Gr}_{1,5}^{>0})^k$ [ELP$^+$23, Proposition 6.22], or equivalently in terms of e.g. $\left(\frac{\beta_i}{\alpha_i}, \frac{\gamma_i}{\alpha_i}, \frac{\delta_i}{\alpha_i}, \frac{\varepsilon_i}{\alpha_i}\right)_{i=1}^k$ in $\mathbb{R}_+^{4k}$. Composing this with $\tilde{Z}^{-1}$ gives a diffeomorphism $g : Z_S^\circ \to \mathbb{R}_+^{4k}$ that sends $Y \in Z_S^\circ$ to the (ratios of) coordinate functionaries $\left(\frac{\beta_i(Y)}{\alpha_i(Y)}, \frac{\gamma_i(Y)}{\alpha_i(Y)}, \frac{\delta_i(Y)}{\alpha_i(Y)}, \frac{\epsilon_i(Y)}{\alpha_i(Y)}\right)_{i=1}^k$. Hence can obtain the candidate canonical

form of the tile Z_S as:

$$\tilde{\Omega}(Z_S) = g^* \bigwedge_{i=1}^{k} \mathrm{dlog}\frac{\beta_i}{\alpha_i} \wedge \mathrm{dlog}\frac{\gamma_i}{\alpha_i} \wedge \mathrm{dlog}\frac{\delta_i}{\alpha_i} \wedge \mathrm{dlog}\frac{\epsilon_i}{\alpha_i} = \bigwedge_{i=1}^{k} \mathrm{dlog}\frac{\beta_i(Y)}{\alpha_i(Y)} \wedge \mathrm{dlog}\frac{\gamma_i(Y)}{\alpha_i(Y)} \wedge \mathrm{dlog}\frac{\delta_i(Y)}{\alpha_i(Y)} \wedge \mathrm{dlog}\frac{\epsilon_i(Y)}{\alpha_i(Y)}.$$

□

Example 7.15. For the BCFW tile $S_{\mathfrak{r}}$ in Figure 6, the coordinate functionaries $\{\zeta_i(Y)\}$ are in Example 3.11. Then we can compute the canonical form of $S_{\mathfrak{r}}$ in terms of $\{\zeta_i(Y)\}$ by Equation (14).

Proposition 7.16 (Canonical form of tiles from tile variables and clusters)**.** *Let Z_D be a standard BCFW tile. Let $\check{\mathbf{x}}(D) = \{\check{\zeta}_i(Y)\}_{i=1}^{4k}$ be its collection of tile variables and $\mathcal{A}(\check{\Sigma}_D)$ its associated cluster algebra as in Definition 6.4. Then the candidate canonical form $\tilde{\Omega}(Z_D)$ of Z_D is given by:*

$$\tilde{\Omega}(Z_D) = \bigwedge_{\check{\zeta}_i(Y) \in \check{\mathbf{x}}(D)} \mathit{dlog}\ \check{\zeta}_i(Y). \tag{15}$$

Moreover, for each fixed cluster $\check{\mathbf{x}} = \{x_i\}_{i=1}^{4k}$ in $\mathcal{A}(\check{\Sigma}_D)$, the form $\tilde{\Omega}(Z_D)$ is given by:

$$\tilde{\Omega}(Z_D) = \bigwedge_{x_i \in \check{\mathbf{x}}} \mathit{dlog}\ x_i(Y). \tag{16}$$

The proof easily follows from Theorem 6.7, and the fact there is a bijection $f : Z_D^\circ \to \mathbb{R}_+^{4k}$ that sends $Y \in Z_D^\circ$ to the collection $\check{\mathbf{x}}(D) = \{\check{\zeta}_i(Y)\}$ of $4k$ tile variables. Each tile variable $\check{\zeta}_i(Y)$ is a signed ratio of cluster variables for $\mathrm{Gr}_{4,n}$, in particular of domino variables $\mathbf{x}(D)$, see Proposition 6.1. The same argument holds if instead of $\check{\mathbf{x}}(D)$, we consider an arbitrary cluster $\check{\mathbf{x}}$ in $\mathcal{A}(\check{\Sigma}_D)$.

Example 7.17. For the BCFW tile Z_D in Figure 7, the tile variables $\check{\zeta}_i(Y)$ were computed in Example 3.12. Then we can compute the candidate canonical form $\tilde{\Omega}(Z_D)$ in terms of $\check{\zeta}_i(Y)$ by Equation (15). Moreover, we can also compute $\tilde{\Omega}(Z_D)$ by using a different cluster obtained e.g. by mutating the tile seed $\check{\Sigma}_D$ at $\check{\varepsilon}_5$, see Figure 19. The collection of cluster variables then would have $\check{\varepsilon}'_5$ instead of $\check{\varepsilon}_5$, where

$$\check{\varepsilon}'_5 = \frac{\langle ABC\,|\,89\,|\,DEF\rangle}{\hat{\gamma}_5\hat{\gamma}_6} = \frac{\langle ABC\,|\,89\,|\,DEF\rangle}{\langle 8\ 9\ A\ D\rangle\langle 8\ 9\ E\ F\rangle}$$

and we use A, B, C, D, E, F for $10, 11, 12, 13, 14, 15$. Note that any sequence of mutations applied to $\check{\Sigma}_D$ will give cluster variables which are cluster variables for $\mathrm{Gr}_{4,n}$ times a Laurent monomial in the $\hat{\gamma}_i$.

Appendix A. List of tiles in a spurion tiling

A good tiling $\mathcal{T}_{sp} = \{Z_\pi\}$ for $\mathcal{A}_{9,2,4}$ containing a spurion tile (#28 in the list). For each tile Z_π we display its affine permutation π and the vector configuration of the columns of a matrix C_π representing a point in S_π, where columns within the same bracket $(\dots)$ are proportional.

#	Affine Permutation	Vector Conf.	#	Affine Permutation	Vector Conf.
1	$\{1,4,5,6,7,11,12,8,9\}$	$(2)(3)(4)(5)(6)(7)$	26	$\{2,5,4,9,6,8,7,10,12\}$	$(1,2)(3,4)(5,6,8)(9)$
2	$\{1,4,5,7,6,8,12,11,9\}$	$(8,2)(3)(4)(5,6)(7)$	27	$\{2,6,4,5,7,9,12,8,10\}$	$(3,4,5)(6)(7)(9,1,2)$
3	$\{1,4,5,7,8,6,11,12,9\}$	$(2)(3)(4)(5)(7)(8)$	28	$\{2,6,4,5,9,7,8,12,10\}$	$(3,4,5)(6,7,8)(9,1,2)$
4	$\{1,4,5,8,6,7,12,9,11\}$	$(8,9,2)(3)(4)(5,6,7)$	29	$\{2,7,4,5,6,8,12,9,10\}$	$(3,4,5,6)(7)(8,9,1,2)$
5	$\{1,4,5,8,7,6,9,12,11\}$	$(9,2)(3)(4)(5,7)(8)$	30	$\{2,7,4,5,8,6,9,12,10\}$	$(3,4,5)(7)(8)(9,1,2)$
6	$\{1,4,5,8,9,6,7,11,12\}$	$(2)(3)(4)(5)(8)(9)$	31	$\{3,4,5,9,10,6,7,8,11\}$	$(1)(2)(3)(4)(5)(9)$
7	$\{1,5,3,6,7,8,11,13,9\}$	$(2)(4)(5)(6)(7)(8)$	32	$\{3,5,4,6,10,9,7,8,11\}$	$(1)(2)(3,4)(5)(6,9)$
8	$\{1,5,3,6,8,7,9,13,11\}$	$(9,2)(4)(5)(6,7)(8)$	33	$\{3,5,6,4,9,10,7,8,11\}$	$(1)(2)(3)(5)(6)(9)$
9	$\{1,5,3,6,8,9,7,11,13\}$	$(2)(4)(5)(6)(8)(9)$	34	$\{3,6,4,5,9,8,7,11,10\}$	$(9,1)(2)(3,4,5)(6,8)$
10	$\{1,5,4,6,7,11,8,12,9\}$	$(2)(3,4)(5)(6)(7,8)$	35	$\{3,6,4,5,10,7,8,11,9\}$	$(1)(2)(3,4,5)(6,7,8)$
11	$\{1,5,4,6,8,11,7,9,12\}$	$(2)(3,4)(5)(6)(8,9)$	36	$\{3,6,4,9,5,8,7,10,11\}$	$(1)(2)(3,4)(6,8)(9)$
12	$\{1,5,4,7,6,8,11,12,9\}$	$(2)(3,4)(5,6)(7)(8)$	37	$\{3,6,5,4,7,8,11,10,9\}$	$(8,1)(2)(3,5)(6)(7)$
13	$\{1,5,4,8,6,7,9,12,11\}$	$(3,4)(5,6,7)(8)(9,2)$	38	$\{3,6,5,4,8,7,11,9,10\}$	$(8,9,1)(2)(3,5)(6,7)$
14	$\{1,5,4,8,6,9,7,11,12\}$	$(2)(3,4)(5,6)(8)(9)$	39	$\{3,6,5,4,9,7,8,11,10\}$	$(9,1)(2)(3,5)(6,7,8)$
15	$\{1,6,3,4,7,8,9,11,14\}$	$(2)(5)(6)(7)(8)(9)$	40	$\{3,7,5,4,8,6,9,11,10\}$	$(9,1)(2)(3,5)(7)(8)$
16	$\{1,6,4,5,7,8,12,9,11\}$	$(3,4,5)(6)(7)(8,9,2)$	41	$\{4,6,3,5,9,8,7,10,11\}$	$(1)(2)(4,5)(6,8)(9)$
17	$\{1,6,4,5,8,7,9,12,11\}$	$(3,4,5)(6,7)(8)(9,2)$	42	$\{5,6,3,4,7,9,8,11,10\}$	$(9,1)(2)(5)(6)(7,8)$
18	$\{1,6,5,4,8,7,9,11,12\}$	$(2)(3,5)(6,7)(8)(9)$	43	$\{5,6,3,4,8,9,7,10,11\}$	$(1)(2)(5)(6)(8)(9)$
19	$\{2,3,5,9,6,7,8,13,10\}$	$(9,1,2,3)(4)(5,6,7,8)$	44	$\{5,7,3,4,6,8,9,11,10\}$	$(9,1)(2)(5,6)(7)(8)$
20	$\{2,4,5,9,6,8,7,12,10\}$	$(9,1,2)(3)(4)(5,6,8)$	45	$\{6,3,4,5,9,7,8,11,10\}$	$(2,3,4,5)(6,7,8)(9,1)$
21	$\{2,4,5,9,8,6,7,10,12\}$	$(1,2)(3)(4)(5,8)(9)$	46	$\{6,3,4,9,5,7,8,10,11\}$	$(1)(2,3,4)(6,7,8)(9)$
22	$\{2,4,6,9,5,7,8,12,10\}$	$(9,1,2)(3)(4)(6,7,8)$	47	$\{6,3,5,4,7,8,11,9,10\}$	$(2,3,5)(6)(7)(8,9,1)$
23	$\{2,5,3,6,9,7,8,13,10\}$	$(9,1,2)(4)(5)(6,7,8)$	48	$\{6,4,3,5,9,7,8,10,11\}$	$(1)(2,4,5)(6,7,8)(9)$
24	$\{2,5,3,6,9,8,7,10,13\}$	$(1,2)(4)(5)(6,8)(9)$	49	$\{6,5,3,4,7,9,8,10,11\}$	$(1)(2,5)(6)(7,8)(9)$
25	$\{2,5,4,6,9,10,7,8,12\}$	$(1,2)(3,4)(5)(6)(9)$	50	$\{6,7,3,4,5,8,9,10,11\}$	$(1)(2)(6)(7)(8)(9)$

Substituting the 5 tiles $\#28, 34, 35, 38, 46$ in $\mathcal{T}_{sp}$ with 5 tiles in the table below, we obtain a good BCFW tiling $\mathcal{T}_{BCFW}$.

Affine Permutation	Vector Conf.
$\{1,6,4,5,9,7,8,11,12\}$	$(2)(3,4,5)(6,7,8)(9)$
$\{3,6,4,5,9,7,11,8,10\}$	$(9,1)(2)(3,4,5)(6,7)$
$\{3,6,4,9,5,7,8,11,10\}$	$(9,1)(2)(3,4)(6,7,8)$
$\{3,7,4,5,9,6,8,11,10\}$	$(9,1)(2)(3,4,5)(7,8)$
$\{4,6,3,5,9,7,8,11,10\}$	$(9,1)(2)(4,5)(6,7,8)$

References

[AHBC+16a] Nima Arkani-Hamed, Jacob Bourjaily, Freddy Cachazo, Alexander Goncharov, Alexander Postnikov, and Jaroslav Trnka. *Grassmannian geometry of scattering amplitudes*. Cambridge University Press, Cambridge, 2016.

[AHBC+16b] Nima Arkani-Hamed, Jacob L. Bourjaily, Freddy Cachazo, Alexander B. Goncharov, Alexander Postnikov, and Jaroslav Trnka. *Grassmannian Geometry of Scattering Amplitudes*. Cambridge University Press, 4 2016.

[AHBL17] Nima Arkani-Hamed, Yuntao Bai, and Thomas Lam. Positive Geometries and Canonical Forms. *JHEP*, 11:039, 2017.

[AHCCK10] Nima Arkani-Hamed, Freddy Cachazo, Clifford Cheung, and Jared Kaplan. A Duality For The S Matrix. *JHEP*, 03:020, 2010.

[AHT14] Nima Arkani-Hamed and Jaroslav Trnka. The amplituhedron. *J. High Energy Phys.*, 10:33, 2014.

[ELP+23] Chaim Even-Zohar, Tsviqa Lakrec, Matteo Parisi, Ran Tessler, Melissa Sherman-Bennett, and Lauren Williams. Cluster algebras and tilings for the m= 4 amplituhedron. *arXiv preprint arXiv:2310.17727*, 2023.

[ELT21] Chaim Even-Zohar, Tsviqa Lakrec, and Ran J Tessler. The amplituhedron bcfw triangulation. *full version of preprint arXiv:2112.02703*, 2021.

[Fra16] Chris Fraser. Quasi-homomorphisms of cluster algebras. *Adv. in Appl. Math.*, 81:40–77, 2016.

[GL20] Pavel Galashin and Thomas Lam. Parity duality for the amplituhedron. *Compositio Mathematica*, 156(11):2207–2262, 2020.

[GLS13] Christof Geiss, Bernard Leclerc, and Jan Schröer. Factorial cluster algebras. *Doc. Math.*, 18:249–274, 2013.

[GP23] Ömer Gürdoğan and Matteo Parisi. Cluster patterns in Landau and leading singularities via the amplituhedron. *Ann. Inst. Henri Poincaré D*, 10(2):299–336, 2023.

[Hod13] Andrew Hodges. Eliminating spurious poles from gauge-theoretic amplitudes. *J. High Energy Phys.*, (135), 2013.

[KLS13] Allen Knutson, Thomas Lam, and David E. Speyer. Positroid varieties: juggling and geometry. *Compos. Math.*, 149(10):1710–1752, 2013.

[KPR+21] Kathlén Kohn, Ragni Piene, Kristian Ranestad, Felix Rydell, Boris Shapiro, Rainer Sinn, Miruna-Stefana Sorea, and Simon Telen. Adjoints and canonical forms of polypols, 2021.

[KR20] Kathlén Kohn and Kristian Ranestad. Projective geometry of Wachspress coordinates. *Found. Comput. Math.*, 20(5):1135–1173, 2020.

[KW19] Steven N. Karp and Lauren K. Williams. The $m = 1$ amplituhedron and cyclic hyperplane arrangements. *Int. Math. Res. Not. IMRN*, 5:1401–1462, 2019.

[KWZ20] Steven N Karp, Lauren K Williams, and Yan X Zhang. Decompositions of amplituhedra. *Annales de l'Institut Henri Poincaré D*, 7(3):303–363, 2020.

[Lam22] Thomas Lam. An invitation to positive geometries. 8 2022.

[Lus94] G. Lusztig. Total positivity in reductive groups. In *Lie theory and geometry*, volume 123 of *Progr. Math.*, pages 531–568. Birkhäuser Boston, Boston, MA, 1994.

[MS09] L. J. Mason and David Skinner. Dual Superconformal Invariance, Momentum Twistors and Grassmannians. *JHEP*, 11:045, 2009.

[MS17] Greg Muller and David E. Speyer. The twist for positroid varieties. *Proc. Lond. Math. Soc. (3)*, 115(5):1014–1071, 2017.

[Pos06] Alexander Postnikov. Total positivity, Grassmannians, and networks. *arXiv:math/0609764*, 2006.

Faculty of Mathematics, Technion, Haifa, Israel
Email address: chaime@technion.ac.il

Institute of Mathematics, University of Zurich, Switzerland
Email address: tsviqa@gmail.com

CMSA, Harvard University, Cambridge, MA; Institute for Advanced Study, Princeton, NJ;
Email address: mparisi@cmsa.fas.harvard.edu

Department of Mathematics, MIT, Cambridge, MA
Email address: msherben@mit.edu

Department of Mathematics, Weizmann Institute of Science, Israel
Email address: ran.tessler@weizmann.ac.il

Department of Mathematics, Harvard University, Cambridge, MA
Email address: williams@math.harvard.edu